

Limited Feedback Beamforming Systems for Dual-Polarized MIMO Channels

Taejoon Kim, *Student Member, IEEE*, Bruno Clerckx, *Member, IEEE*, David J. Love, *Senior Member, IEEE*, and Sung Jin Kim, *Member, IEEE*

Abstract—Dual-polarized multiple-input multiple-output (MIMO) antenna systems, where the antennas are grouped in pairs of orthogonally polarized antennas, are a spatially-efficient alternative to single polarized MIMO antenna systems. A limited feedback beamforming technique is proposed for dual-polarized MIMO channels where the receiver has perfect channel knowledge but the transmitter only receives partial information regarding the channel instantiation. The system employs an effective signal-to-noise ratio (SNR) distortion minimizing codebook to convey channel state information (CSI) in the form of beamforming direction. By investigating the average SNR performance of this system, an upper bound on the average SNR distortion is found as a weighted sum of two beamforming distortion metrics. The distortion minimization problem is solved by designing a concatenated codebook. Finally, we propose a codebook switching scheme exploiting the cross-polar discrimination (XPD) statistics. Simulations show that the proposed codebook switching scheme with an XPD dependent concatenated codebook has the ability to adapt to dual-polarized channels.

Index Terms—Dual-polarized channel, multiple-input multiple-output (MIMO) systems, quantized beamforming, codebook design.

I. INTRODUCTION

MULTIPLE-input multiple-output (MIMO) antenna systems have become more and more important with the evolution of next generation and beyond (i.e., 4G and beyond) broadband wireless standards that support high data rates and high performance [1]. In order to obtain the maximum capacity and reliability benefits available in MIMO wireless systems, it is usually required that the antennas are spaced at least a half wavelength at the subscriber unit and at least ten wavelengths at the base station [2]. However, device space limitations do not allow large spacing at either side. One solution to decreasing the necessary physical space needed is to employ dual-polarized antennas, where the antennas are grouped in pairs of polarized collocated antennas.

Manuscript received May 22, 2009; revised November 13, 2009 and April 16, 2010; accepted June 16, 2010. The associate editor coordinating the review of this paper and approving it for publication was M. Shafi.

T. Kim and D. J. Love are with the School of Electrical and Computer Engineering, Purdue University, West Lafayette, IN, 47906 USA (e-mail: {kim487, djlove}@ecn.purdue.edu).

B. Clerckx and S. J. Kim are with Samsung Advanced Institute of Technology, Samsung Electronics, Yongin-Si, Gyeonggi-Do, 446-712 Korea (e-mail: {bruno.clerckx, communication}@samsung.com).

This work was supported in part by Samsung and by the Doctoral Fellowship Program funded by the Korean government (MOCIE). The materials in this paper were presented in part at the IEEE Globecom Conference, New Orleans, LA, December 2008.

Digital Object Identifier 10.1109/TWC.2010.09.090754

Unfortunately, the different orthogonal polarizations of the dual-polarized antenna systems result in complicated properties. Much work has been aimed at modeling and analyzing the coupling of dual-polarized MIMO channels [2]–[6]. In [3], measured data was used to show that the capacity varies significantly with channel imperfection such as delay spread, Ricean K -factor, and cross-polar discrimination (XPD). The performance of spatial multiplexing and space-time block coding (e.g., Alamouti coding) in MIMO dual-polarized antenna systems has been investigated in [4]. In [2], a dual-polarized channel is modeled using a vector geometrical scattering mechanism. Spatially separated dual-polarized MIMO channels are modeled in [5], and the insensitivity of performance to channel imperfections compared to the single polarized channel is emphasized. Based on measured data, [6] and [7] conclude that the mean value of the XPD variable for MIMO channels evolves from 5 dB to 15 dB, and when the channel has a large K -factor, dual-polarized antennas provide robust isolation between orthogonal polarizations.

Closed-loop MIMO signaling techniques such as beamforming and spatial multiplexing require knowledge of the channel state information (CSI) at the transmitter [8]. Acquisition of CSI at the transmitter in frequency division duplexing (FDD) systems is challenging, because the uplink channel realization is normally independent of the downlink channel realization. Thus, a feedback link from the receiver to the transmitter is required to provide the transmitter with CSI. In theory, acquisition of CSI at the transmitter is available in time division duplexing (TDD) systems by using the channel reciprocity between uplink and downlink. However, in practice, tight RF chain calibration is required at the transmitter and receiver to accomplish this TDD reciprocity across the entire analog signal path [9]. Thus, the utility of the feedback is not restricted to FDD systems only. To meet the bandwidth requirement of the feedback channel, limited feedback techniques have been considered for MIMO channels (e.g., [9]–[13]). Limited feedback MIMO schemes dealing with transmit spatial correlation have also been studied [14], [15]. In these limited feedback systems, the receiver sends to the transmitter an index of the transmit beamformer chosen in a finite-set vector codebook common to the transmitter and the receiver. The transmitter uses this feedback to direct the beam to the receiver.

For dual-polarized MIMO channels, designing an optimal beamforming codebook matched to the channel statistics is not tractable due to the power leakage between different po-

larizations. Only limited work has been published on codebook designs for dual-polarized systems [16], [17]. An approach for precoding codebook design in dual-polarized MIMO channels has been proposed in [16]. In [17], an intuitive concatenated codebook approach has been proposed for a beamforming system.

In this paper, a framework for limited feedback beamforming and combining in MIMO dual-polarized channels is proposed that assumes the transmitter and receiver both know the XPD variable. This can be accomplished by having the receiver measure the XPD and share this long term statistic with the transmitter. In beamforming and combining systems, it has been shown that the beamformer and combiner must be chosen to maximize the effective SNR in order to minimize the average symbol error rate and maximize the capacity [18], [19]. Thus, following the analysis in [10], [12]–[15], we use the average SNR distortion as a performance metric to design the limited feedback system. Here, we extend the basic intuition on the concatenated codebook discussed in the conference version [17] of this paper. However, different from [17], we propose a rigorous and complete framework to design and use limited feedback in dual-polarized MIMO channels. First, the average SNR distortion metric is analyzed and useful properties are derived. This analysis allows us to derive a tractable upper bound on the average SNR distortion. Next, the effects of XPD variation on the average SNR distortion are studied. This motivates our proposed concatenated codebook switching method. The distortion upper bound of the concatenated codebook switching scheme is minimized by adjusting the allocation of the codewords between different codebooks. The key analytical tool used to solve the minimization problem is a random vector quantization (RVQ) argument that enables closed-form solutions to the codeword allocation problem. In order to provide clear insight about the behavior of the proposed scheme, asymptotic analysis is carried out. Finally, the performance of the proposed algorithm is verified by extensive simulation study.

The paper is organized as follows. In Section II, we describe the limited feedback system model in dual-polarized MIMO channels. The performance metric is defined and a tractable performance bound is obtained in Section III. In Section IV, a codebook structure that can adapt to the XPD variable of the channel is defined, and in Section V, the codebook design problem is solved by minimizing the distortion bound. Simulation results to verify the analysis and performance are given in Section VI, and we close by discussing conclusions in Section VII.

Notation: A boldcase capital letter \mathbf{A} denotes a matrix, a bold lowercase letter \mathbf{a} denotes a vector, T denotes a transpose, $*$ denotes a conjugate transpose, $\|\mathbf{a}\|_2$ denotes a vector two norm, $\lambda_k(\mathbf{A}^* \mathbf{A})$ denotes the k -th dominant eigenvalue of the matrix $\mathbf{A}^* \mathbf{A}$, \odot denotes the Hadamard product, \otimes denotes the Kronecker product, $\mathbf{1}_{M \times N}$ and $\mathbf{0}_{M \times N}$ denote the M by N matrices with all 1 entries and the M by N matrices with all 0 entries, respectively, and r.h.s. and l.h.s. denote the right hand side and the left hand side, respectively. If \mathcal{A} denotes a set, $\text{car}(\mathcal{A})$ denotes the cardinality of \mathcal{A} , and a function $f(x) : [a, b] \rightarrow \mathbb{R}$ is called a monotonically increasing function on $[a, b]$ if $a \leq x_1 \leq x_2 \leq b$ implies $f(x_1) \leq f(x_2)$.

II. SYSTEM MODEL

Consider a MIMO wireless system employing limited feedback transmit beamforming and receive combining. The transmitter and receiver employ M_t transmit antennas and M_r receive antennas, respectively. Because we assume dual-polarized antennas, M_t and M_r are assumed to be even numbers. The antenna configuration is shown in Fig. 1, where the V-Ant. denotes the antenna with vertical (V) polarization and H-Ant. denote the antenna with horizontal (H) polarization, respectively.

With the flat fading assumption, the channel matrix is depicted by an input-output relation with V to V, V to H, H to H, and H to V polarized waves. For example, a 4×4 dual-polarized channel matrix can be expressed as

$$\mathbf{H} = \begin{bmatrix} h_{11,VV} & h_{12,VV} & h_{13,VH} & h_{14,VH} \\ h_{21,VV} & h_{22,VV} & h_{23,VH} & h_{24,VH} \\ h_{31,HV} & h_{32,HV} & h_{33,HH} & h_{34,HH} \\ h_{41,HV} & h_{42,HV} & h_{43,HH} & h_{44,HH} \end{bmatrix}. \quad (1)$$

The $h_{ij,P_i P_j}$ in (1) denotes the fading element from the j -th transmit antenna with P_j polarization to the i -th receive antenna with P_i polarization where $P_i, P_j \in \{V, H\}$. In Fig. 1, the 4×4 dual-polarized MIMO system has two spatially separated dual-polarized antennas at each side, where the first dual-polarized antenna is formed by grouping the first antenna with V polarization and the third antenna with H polarization in pairs, and the second dual-polarized antenna is formed by grouping the second V antenna and the fourth H antenna.

The received signal is represented as

$$y = \sqrt{\rho} \mathbf{z}^* \mathbf{H}_\chi \mathbf{f} s + \mathbf{z}^* \mathbf{n}. \quad (2)$$

The vectors $\mathbf{z} \in \mathbb{C}^{M_r \times 1}$ and $\mathbf{f} \in \mathbb{C}^{M_t \times 1}$ represent the unit-norm (i.e., $\|\mathbf{z}\|_2 = \|\mathbf{f}\|_2 = 1$) receive combining and transmit beamforming vectors, respectively. The noise vector $\mathbf{n} \in \mathbb{C}^{M_r \times 1}$ has independent and identically distributed (i.i.d.) entries with normal distribution $\mathcal{CN}(0, 1)$, s represents the transmitted symbol whose energy is $E_s[|s|^2] = 1$, and ρ is the signal to noise ratio (SNR). The channel $\mathbf{H}_\chi \in \mathbb{C}^{M_r \times M_t}$ is a dual-polarized MIMO channel parameterized by the single parameter χ that is assumed to be modeled by [20]

$$\mathbf{H}_\chi = \mathbf{X} \odot \mathbf{H}_w, \quad (3)$$

where $\mathbf{H}_w \in \mathbb{C}^{M_r \times M_t}$ denotes a single polarized channel having i.i.d. entries with $\mathcal{CN}(0, 1)$. The term ‘‘single polarized channel’’ is used to represent a channel inducing no power imbalance between the channel elements, i.e., all channel elements have unit power. $\mathbf{X} \in \mathbb{C}^{M_r \times M_t}$ is a matrix describing the power imbalance between the orthogonal polarizations. It is modeled as

$$\mathbf{X} = \begin{bmatrix} 1 & \sqrt{\chi} \\ \sqrt{\chi} & 1 \end{bmatrix} \otimes \mathbf{1}_{\frac{M_r}{2} \times \frac{M_t}{2}}. \quad (4)$$

The parameter $0 \leq \chi \leq 1$ stands for the inverse of the XPD, where $1 \leq \text{XPD} \leq \infty$. The XPD refers to the physical ability of the antennas to distinguish the orthogonal polarization. Then, the Hadamard product of \mathbf{X} and \mathbf{H}_w in (3) gives a block matrix representation

$$\mathbf{H}_\chi = \begin{bmatrix} \mathbf{H}_{w,11} & \sqrt{\chi} \mathbf{H}_{w,12} \\ \sqrt{\chi} \mathbf{H}_{w,21} & \mathbf{H}_{w,22} \end{bmatrix}. \quad (5)$$

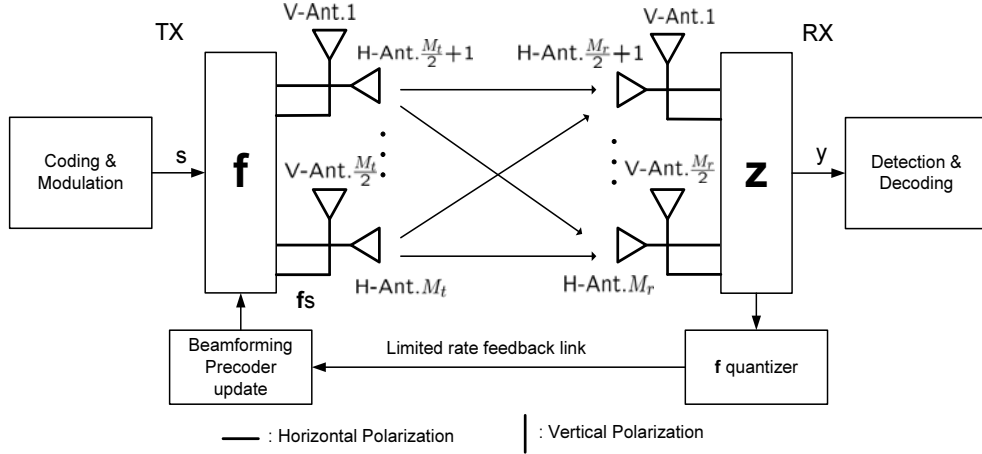


Fig. 1. Block diagram of an $M_r \times M_t$ dual-polarized channel MIMO system.

In (5), the $\mathbf{H}_{w,ij}$ for $1 \leq i, j \leq 2$ is formed by taking rows from $(M_r(i-1)/2) + 1$ to $M_r(i/2)$ and columns from $(M_t(j-1)/2) + 1$ to $M_t(j/2)$ of \mathbf{H}_w having i.i.d. entries distributed as $\mathcal{CN}(0, 1)$. Note that $\mathbf{H}_{w,11}$ and $\mathbf{H}_{w,22}$ correspond to co-polarized components, and $\sqrt{\chi}\mathbf{H}_{w,12}$ and $\sqrt{\chi}\mathbf{H}_{w,21}$ correspond to cross-polarized components. Here, we assume that the amounts of power coupling from V to H and from H to V are the same. This symmetry assumption is motivated by the work in [2], [4], [5], [7], [20]. The model in (5) is matched well for line-of-sight (LOS) propagation conditions. When there are non-LOS (NLOS) or LOS with low K -factor conditions, the dual-polarized channel can be effectively modeled by encompassing the effect of the polarization rotation [21], [22].

The receive SNR after combining is called the effective SNR and is given by

$$\gamma_r = \rho |\mathbf{z}^* \mathbf{H}_\chi \mathbf{f}|^2.$$

We assume a maximal-ratio combiner (MRC) is used at the receiver (i.e., $\mathbf{z} = \mathbf{H}_\chi \mathbf{f} / \|\mathbf{H}_\chi \mathbf{f}\|_2$) where the MRC weight is aimed to maximize γ_r yielding $\gamma_r = \rho \|\mathbf{H}_\chi \mathbf{f}\|_2^2$. In the limited feedback beamforming system, assuming ideal channel estimation, the receiver determines the best beamforming vector \mathbf{f}_{opt} among $N=2^B$ codewords in the codebook $\mathcal{F} = \{\mathbf{f}_1, \mathbf{f}_2, \dots, \mathbf{f}_N\}$ so that it maximizes γ_r , i.e., $\mathbf{f}_{opt} = \underset{1 \leq k \leq N}{\operatorname{argmax}} \|\mathbf{H}_\chi \mathbf{f}_k\|_2^2$. The codebook \mathcal{F} is known to both the transmitter and the receiver, and the receiver reports the index of \mathbf{f}_{opt} to the transmitter. By selecting the transmit beamforming vector codeword with respect to (w.r.t.) the feedback index, transmit beamforming is performed. The codebook \mathcal{F} is optimized using a system performance metric that will be introduced in the next few sections. Throughout the paper, we use the notation \mathcal{Q} to denote the optimized \mathcal{F} .

III. AVERAGE DISTORTION AND PERFORMANCE BOUND

In this section, we analyze the performance averaged over the fading distribution. The average SNR distortion metric is employed to measure the performance loss due to the quantization. A tractable upper bound of the average SNR distortion for designing the distortion minimizing codebook is derived.

It is helpful to decompose the channel \mathbf{H}_χ using a block diagonal matrix \mathbf{H}_d and off-block diagonal matrix \mathbf{H}_{od} as

$$\begin{aligned} \mathbf{H}_\chi &= \mathbf{H}_d + \sqrt{\chi} \mathbf{H}_{od} \\ &\triangleq \begin{bmatrix} \mathbf{H}_{w,11} & \mathbf{0}_{\frac{M_r}{2} \times \frac{M_t}{2}} \\ \mathbf{0}_{\frac{M_r}{2} \times \frac{M_t}{2}} & \mathbf{H}_{w,22} \end{bmatrix} + \sqrt{\chi} \begin{bmatrix} \mathbf{0}_{\frac{M_r}{2} \times \frac{M_t}{2}} & \mathbf{H}_{w,12} \\ \mathbf{H}_{w,21} & \mathbf{0}_{\frac{M_r}{2} \times \frac{M_t}{2}} \end{bmatrix}. \end{aligned} \quad (6)$$

As a performance metric, we use the average effective SNR, i.e., $E \left[\max_{\mathbf{f} \in \mathcal{F}} \|\mathbf{H}_\chi \mathbf{f}\|_2^2 \right]$. Our goal is to design a codebook $\mathcal{F} = \{\mathbf{f}_1, \mathbf{f}_2, \dots, \mathbf{f}_N\}$ to maximize the objective function $E \left[\max_{\mathbf{f} \in \mathcal{F}} \|\mathbf{H}_\chi \mathbf{f}\|_2^2 \right]$. Maximizing the objective function is equivalent to minimizing

$$G(\mathcal{F}, \chi) = E \left[\lambda_1(\mathbf{H}_\chi^* \mathbf{H}_\chi) \right] - E \left[\max_{\mathbf{f} \in \mathcal{F}} \|\mathbf{H}_\chi \mathbf{f}\|_2^2 \right], \quad (8)$$

which represents the average SNR loss due to the quantization. To facilitate the analysis, in the sequel, given the codeword set $\mathcal{F} = \{\mathbf{f}_1, \mathbf{f}_2, \dots, \mathbf{f}_N\}$, we define the Voronoi region associated with the codeword \mathbf{f}_n as the set of all channel matrices closer to \mathbf{f}_n than the other codeword \mathbf{f}_m ($m \neq n$), i.e.,

$$\mathcal{V}_{\chi, n} = \{ \mathbf{H}_\chi : \|\mathbf{H}_\chi \mathbf{f}_n\|_2^2 \geq \|\mathbf{H}_\chi \mathbf{f}_m\|_2^2 \forall m \neq n, 1 \leq m \leq N \}. \quad (9)$$

In order to analyze the performance, we will have to understand the statistics of $\mathbf{H}_\chi^* \mathbf{H}_\chi$. Using (6), we can expand $\mathbf{H}_\chi^* \mathbf{H}_\chi$ as

$$\mathbf{H}_\chi^* \mathbf{H}_\chi = \mathbf{H}_d^* \mathbf{H}_d + \chi \mathbf{H}_{od}^* \mathbf{H}_{od} + \sqrt{\chi} \mathbf{R}_c, \quad (10)$$

where $\mathbf{R}_c = \mathbf{H}_d^* \mathbf{H}_{od} + \mathbf{H}_{od}^* \mathbf{H}_d$ denotes a symmetric off-block diagonal matrix. In addition, we define a dual-polarized channel with an arbitrary variation $\sqrt{\chi} \Delta$ added to $\sqrt{\chi}$ as

$$\mathbf{H}_{\chi+\Delta} \triangleq \begin{bmatrix} \mathbf{H}_{w,11} & \sqrt{\chi}(1+\Delta)\mathbf{H}_{w,12} \\ \sqrt{\chi}(1+\Delta)\mathbf{H}_{w,21} & \mathbf{H}_{w,22} \end{bmatrix} \quad (11)$$

where $0 \leq \Delta \leq \frac{1-\sqrt{\chi}}{\sqrt{\chi}}$. Note that when $\Delta=0$, $\mathbf{H}_{\chi+\Delta}$ becomes \mathbf{H}_χ and when $\Delta = \frac{1-\sqrt{\chi}}{\sqrt{\chi}}$, $\mathbf{H}_{\chi+\Delta}$ equals \mathbf{H}_1 . This definition will be found to be useful in the later derivations. With the above definitions, we establish a monotonicity of $\lambda_1(\mathbf{H}_\chi^* \mathbf{H}_\chi)$ on χ as below.

Lemma 1: Given a single realization of \mathbf{H}_w , for $\chi \in [0, 1]$, the dominant eigenvalues of $\mathbf{H}_\chi^* \mathbf{H}_\chi$ and $\mathbf{H}_{\chi+\Delta}^* \mathbf{H}_{\chi+\Delta}$, both defined according to (11), satisfy $\lambda_1(\mathbf{H}_\chi^* \mathbf{H}_\chi) \leq \lambda_1(\mathbf{H}_{\chi+\Delta}^* \mathbf{H}_{\chi+\Delta})$ for $0 \leq \Delta \leq \frac{1-\sqrt{\chi}}{\sqrt{\chi}}$. This asserts that $\lambda_1(\mathbf{H}_\chi^* \mathbf{H}_\chi)$ is a monotonic increasing function of χ .

Proof: See Appendix A. ■

From Lemma 1, it is obvious to state that $E[\lambda_1(\mathbf{H}_\chi^* \mathbf{H}_\chi)]$ is also a monotonic increasing function of χ . We next establish the monotonicity of $E\left[\max_{\mathbf{f} \in \mathcal{F}} \|\mathbf{H}_\chi \mathbf{f}\|_2^2\right]$ below.

Lemma 2: For $\chi \in [0, 1]$, $E\left[\max_{\mathbf{f} \in \mathcal{F}} \|\mathbf{H}_\chi \mathbf{f}\|_2^2\right]$ is a monotonic increasing function of χ . Thus, $E\left[\max_{\mathbf{f} \in \mathcal{F}} \|\mathbf{H}_\chi \mathbf{f}\|_2^2\right] \leq E\left[\max_{\mathbf{f} \in \mathcal{F}} \|\mathbf{H}_{\chi+\Delta} \mathbf{f}\|_2^2\right]$ with $0 \leq \Delta \leq \frac{1-\sqrt{\chi}}{\sqrt{\chi}}$.

Proof: See Appendix B. ■

From Lemma 1 and Lemma 2, we establish the monotonicity of $E[\lambda_1(\mathbf{H}_\chi^* \mathbf{H}_\chi)]$ and $E\left[\max_{\mathbf{f} \in \mathcal{F}} \|\mathbf{H}_\chi \mathbf{f}\|_2^2\right]$ on the χ axis. Now, we expand these results to establish that the average SNR distortion $G(\mathcal{F}, \chi)$ is also monotonic and even a convex function on $\sqrt{\chi}$.

Theorem 1: The average SNR distortion $G(\mathcal{F}, \chi)$, where the beamforming codeword is chosen in the finite element codebook \mathcal{F} , is a monotonically increasing convex function of $\sqrt{\chi}$ for $0 \leq \chi \leq 1$.

Proof: See Appendix C. ■

Unfortunately, directly working with $G(\mathcal{F}, \chi)$ when designing a codebook is impractical. Alternatively, we derive a tractable upper bound of $G(\mathcal{F}, \chi)$ and optimize the codebook by minimizing this upper bound.

Corollary 1: The average SNR distortion $G(\mathcal{F}, \chi)$ is upper bounded by

$$G(\mathcal{F}, \chi) \leq \sqrt{\chi} E\left[\lambda_1(\mathbf{H}_w^* \mathbf{H}_w) - \max_{\mathbf{f} \in \mathcal{F}} \|\mathbf{H}_w \mathbf{f}\|_2^2\right] + (1 - \sqrt{\chi}) E\left[\lambda_1(\mathbf{H}_d^* \mathbf{H}_d) - \max_{\mathbf{f} \in \mathcal{F}} \|\mathbf{H}_d \mathbf{f}\|_2^2\right]. \quad (12)$$

Proof: For any convex function $h(x)$ over an interval $x \in [a, b]$, the definition of the convex function gives

$$h(x) = h\left(\frac{x-a}{b-a} b + \frac{b-x}{b-a} a\right) \leq \frac{x-a}{b-a} h(b) + \frac{b-x}{b-a} h(a). \quad (13)$$

Applying (13) to $G(\mathcal{F}, \chi)$ over the interval $\sqrt{\chi} \in [0, 1]$ gives (12). ■

Now, $G(\mathcal{F}, \chi)$ is upper bounded by the weighted sum of the average SNR loss for a single polarized channel and average SNR loss for a block diagonal channel.

Before we proceed to the codebook design details, we address the tightness of the bound (12). In (12), we use the definition of the convex function to obtain the upper bound. Usually, the inequality in the definition of the convex function results in a trivial bound unless the function is monotone across the interval. However, by Theorem 1, we know that $G(\mathcal{F}, \chi)$ is a monotonically increasing function which implies the bound in (12) is a non-trivial upper bound. Also, the bound is quite tight for small and large value of χ . The inequality becomes equality for the particular values of $\chi = 0$ and $\chi = 1$.

For values of χ between 0 and 1, directly arguing the tightness of the bound requires closed-form solutions of the quantities at the r.h.s. of (12) which are in general unknown. However, as we will show in the simulation study of the resulting codebook design, the bound in (12) closely models the average SNR distortion in (8).

IV. CONCATENATED CODEBOOK STRUCTURE

In our system setup, we have assumed the scenario where the receiver can measure the long term statistic χ and share this information with the transmitter so that the codebook \mathcal{F} can be adapted to the current channel XPD. We assume the overhead required to send χ is negligible. In this section, we define a concatenated codebook structure that can adapt to the long term statistic χ . This codebook structure is fully motivated by the proposed distortion upper bound in (12).

Before we proceed, consider the two special cases of $\chi = 1$ and $\chi = 0$. When $\chi = 1$, the channel matrix becomes \mathbf{H}_w , i.e., an i.i.d. complex Gaussian matrix. For the channel matrix \mathbf{H}_w , we denote the codebook matched to \mathbf{H}_w as $\mathcal{F}_w = \{\mathbf{f}_{w,1}, \mathbf{f}_{w,2}, \dots, \mathbf{f}_{w,N}\}$. Then, $G(\mathcal{F}_w, 1)$ can be bounded by [12]

$$G(\mathcal{F}_w, 1) = E\left[\lambda_1(\mathbf{H}_w^* \mathbf{H}_w) - \max_{\mathbf{f}_w \in \mathcal{F}_w} \|\mathbf{H}_w \mathbf{f}_w\|_2^2\right] \leq E[\lambda_1(\mathbf{H}_w^* \mathbf{H}_w)] E\left[1 - \max_{\mathbf{f}_w \in \mathcal{F}_w} |\mathbf{v}_{w,1}^* \mathbf{f}_w|^2\right], \quad (14)$$

where $\mathbf{v}_{w,1}$ denotes the dominant eigenvector of $\mathbf{H}_w^* \mathbf{H}_w$, which is isotropically distributed in M_t -dimensional unit norm vector space¹. Thus, the codebook \mathcal{F}_w should be designed by quantizing the random vector space of $\mathbf{v}_{w,1}$ so that (14) is minimized [11], [12]. When $\chi = 0$, the channel matrix becomes block diagonal matrix \mathbf{H}_d . In this case, we denote the codebook matched to \mathbf{H}_d as $\mathcal{F}_d = \{\mathbf{f}_{d,1}, \mathbf{f}_{d,2}, \dots, \mathbf{f}_{d,N}\}$. Then, $G(\mathcal{F}_d, 0)$ can be upper bounded by

$$G(\mathcal{F}_d, 0) = E\left[\lambda_1(\mathbf{H}_d^* \mathbf{H}_d) - \max_{\mathbf{f}_d \in \mathcal{F}_d} \|\mathbf{H}_d \mathbf{f}_d\|_2^2\right] \leq E[\lambda_1(\mathbf{H}_d^* \mathbf{H}_d)] E\left[1 - \max_{\mathbf{f}_d \in \mathcal{F}_d} |\mathbf{v}_{d,1}^* \mathbf{f}_d|^2\right], \quad (15)$$

where $\mathbf{v}_{d,1}$ denotes the dominant eigenvector of $\mathbf{H}_d^* \mathbf{H}_d$. Thus, the codebook \mathcal{F}_d should be designed by quantizing the random vector space of $\mathbf{v}_{d,1}$ so that (15) is minimized. Note that $\mathbf{v}_{d,1}$ has either an upper non-zero structure (i.e., $\mathbf{v}_{d,1} = [\mathbf{v}_{du,1}^T, \mathbf{0}_{1 \times M_t/2}]^T$ where $\mathbf{v}_{du,1}$ is the dominant eigenvector of $\mathbf{H}_{w,11}^* \mathbf{H}_{w,11}$) or a lower non-zero structure (i.e., $\mathbf{v}_{d,1} = [\mathbf{0}_{1 \times M_t/2}, \mathbf{v}_{dl,1}^T]^T$ where $\mathbf{v}_{dl,1}$ is the dominant eigenvector of $\mathbf{H}_{w,22}^* \mathbf{H}_{w,22}$). Hence, an upper non-zero or lower non-zero constraint on any codeword $\mathbf{f}_d \in \mathcal{F}_d$ is necessary to be matched with the channel subspace. We denote \mathcal{F}_d as the block diagonal codebook.

Motivated by the distortion upper bound in (12), the concatenated codebook structure needed to adapt to χ is defined as follows. The distortion minimizing concatenated codebook

¹When there exist antenna correlations, eigenvectors are no longer isotropically distributed. In this case, the impact of the biased eigenvectors on the capacity performance has been studied in [23], which includes the case of dual-polarized channel.

is denoted by $\mathcal{Q} = \{\mathbf{q}_1, \mathbf{q}_1, \dots, \mathbf{q}_N\}$ with $\text{car}(\mathcal{Q}) = N = 2^B$. We also denote $\text{car}(\mathcal{F}_w) = N_w$ and $\text{car}(\mathcal{F}_d) = N_d$, respectively. Then, the size N concatenated codebook \mathcal{Q} is constructed by augmenting the N_w element codebook $\mathcal{F}_w = \{\mathbf{f}_{w,1}, \mathbf{f}_{w,2}, \dots, \mathbf{f}_{w,N_w}\}$ and the N_d element codebook $\mathcal{F}_d = \{\mathbf{f}_{d,1}, \mathbf{f}_{d,2}, \dots, \mathbf{f}_{d,N_d}\}$ (i.e., $\mathcal{Q} = \{\mathcal{F}_w, \mathcal{F}_d\}$ and $N = N_w + N_d$). For notational convenience, we denote $\lambda_1(\mathbf{H}_w^* \mathbf{H}_w)$ and $\lambda_1(\mathbf{H}_d^* \mathbf{H}_d)$ as $\lambda_{w,1}$ and $\lambda_{d,1}$, respectively. By replacing \mathcal{F} with \mathcal{Q} , (12) can be rewritten and upper bounded by

$$\begin{aligned} G(\mathcal{Q}, \chi) &\leq \sqrt{\chi} E \left[\lambda_{w,1} - \max_{\mathbf{q} \in \mathcal{Q}} \|\mathbf{H}_w \mathbf{q}\|_2^2 \right] \\ &\quad + (1 - \sqrt{\chi}) E \left[\lambda_{d,1} - \max_{\mathbf{q} \in \mathcal{Q}} \|\mathbf{H}_d \mathbf{q}\|_2^2 \right] \\ &\leq \sqrt{\chi} E[\lambda_{w,1}] E \left[1 - \max_{\mathbf{q} \in \mathcal{Q}} |\mathbf{v}_{w,1}^* \mathbf{q}|^2 \right] \\ &\quad + (1 - \sqrt{\chi}) E[\lambda_{d,1}] E \left[1 - \max_{\mathbf{q} \in \mathcal{Q}} |\mathbf{v}_{d,1}^* \mathbf{q}|^2 \right] \quad (16) \\ &\leq \sqrt{\chi} E[\lambda_{w,1}] E \left[1 - \max_{\mathbf{f}_w \in \mathcal{F}_w} |\mathbf{v}_{w,1}^* \mathbf{f}_w|^2 \right] \\ &\quad + (1 - \sqrt{\chi}) E[\lambda_{d,1}] E \left[1 - \max_{\mathbf{f}_d \in \mathcal{F}_d} |\mathbf{v}_{d,1}^* \mathbf{f}_d|^2 \right], \quad (17) \end{aligned}$$

where in (17) we use the facts $\text{car}(\mathcal{F}_w) \leq \text{car}(\mathcal{Q})$ and $\text{car}(\mathcal{F}_d) \leq \text{car}(\mathcal{Q})$. Now, our goal is to design the concatenated codebook $\mathcal{Q} = \{\mathcal{F}_w, \mathcal{F}_d\}$ to minimize (17).

A significant amount of work has been done on codebook designs that minimize the first term on the r.h.s. of (17) (e.g., [11], [12]). To enable the design \mathcal{F}_d , we investigate the second term on the r.h.s. of (17). First, we study the structure of \mathcal{F}_d . Let us denote $\mathcal{F}_d = \{\mathcal{F}_{du}, \mathcal{F}_{dl}\} = \{\mathbf{f}_{du,1}, \dots, \mathbf{f}_{du,N_d/2}, \mathbf{f}_{dl,1}, \dots, \mathbf{f}_{dl,N_d/2}\}$ as a codebook consisting of $N_d/2$ upper non-zero codewords \mathbf{f}_{du} and $N_d/2$ lower non-zero codewords \mathbf{f}_{dl} , where N_d is an even positive integer. Having $\text{car}(\mathcal{F}_{du}) = \text{car}(\mathcal{F}_{dl}) = \frac{N_d}{2}$ is obvious because the probability of having upper non-zero or lower non-zero structure for $\mathbf{v}_{d,1}$ is equally likely. Then, the second term on the r.h.s. of (17) is given by

$$\begin{aligned} E \left[1 - \max_{\mathbf{f}_d \in \mathcal{F}_d} |\mathbf{v}_{d,1}^* \mathbf{f}_d|^2 \right] &= \frac{1}{2} E \left[1 - \max_{\mathbf{f}_{du} \in \mathcal{F}_{du}} |\mathbf{v}_{du,1}^* \mathbf{f}_{du}|^2 \right] \\ &\quad + \frac{1}{2} E \left[1 - \max_{\mathbf{f}_{dl} \in \mathcal{F}_{dl}} |\mathbf{v}_{dl,1}^* \mathbf{f}_{dl}|^2 \right]. \quad (18) \end{aligned}$$

Since the eigenvectors $\mathbf{v}_{du,1}$ and $\mathbf{v}_{dl,1}$ are i.i.d., we obtain $E \left[1 - \max_{\mathbf{f}_{du} \in \mathcal{F}_{du}} |\mathbf{v}_{du,1}^* \mathbf{f}_{du}|^2 \right] = E \left[1 - \max_{\mathbf{f}_{dl} \in \mathcal{F}_{dl}} |\mathbf{v}_{dl,1}^* \mathbf{f}_{dl}|^2 \right]$. This allows us to equivalently express (18) as

$$E \left[1 - \max_{\mathbf{f}_d \in \mathcal{F}_d} |\mathbf{v}_{d,1}^* \mathbf{f}_d|^2 \right] = E \left[1 - \max_{\mathbf{f}_s \in \mathcal{F}_s} |\mathbf{v}_{s,1}^* \mathbf{f}_s|^2 \right] \quad (19)$$

where $\mathbf{v}_{s,1}$ denotes the dominant eigenvector of $\mathbf{H}_s^* \mathbf{H}_s$ and \mathbf{H}_s denotes an $M_r/2$ by $M_t/2$ single polarized channel matrix having i.i.d. entries distributed according to $\mathcal{CN}(0, 1)$.

Now, \mathcal{F}_{du} and \mathcal{F}_{dl} are generated by using an $\frac{M_t}{2}$ -dimensional line packing $\mathcal{F}_s = \{\mathbf{f}_{s,1}, \mathbf{f}_{s,2}, \dots, \mathbf{f}_{s,N_d/2}\}$ as the upper and lower non-zero parts, respectively. Using this, the

bound (17) is equivalently rewritten by

$$\begin{aligned} G(\mathcal{Q}, \chi) &\leq \sqrt{\chi} E[\lambda_{w,1}] E \left[1 - \max_{\mathbf{f}_w \in \mathcal{F}_w} |\mathbf{v}_{w,1}^* \mathbf{f}_w|^2 \right] \\ &\quad + (1 - \sqrt{\chi}) E[\lambda_{d,1}] E \left[1 - \max_{\mathbf{f}_s \in \mathcal{F}_s} |\mathbf{v}_{s,1}^* \mathbf{f}_s|^2 \right]. \quad (20) \end{aligned}$$

Note that the bound in (20) is still asymptotically tight in the sense that for a fixed M_t and M_r , as both N_w and N_d tend to infinity the l.h.s. of (20) converges to zero distortion. With the concatenated codebook, the adaptation to χ is performed by adjusting the cardinality of \mathcal{F}_w and \mathcal{F}_d to minimize (20), which will be introduced in the next section.

V. ADAPTATION TO CROSS-POLAR DISCRIMINATION (XPD)

In this section, we design the codebook to minimize the upper bound on the average SNR distortion (20) by exploiting the channel's XPD. The codebook design problem boils down to two optimization problems. The first one is how to pick $N_w = \text{car}(\mathcal{F}_w)$ and $N_d = \text{car}(\mathcal{F}_d)$ to minimize (20). We refer to this as the codeword allocation problem. The second problem (called the concatenation problem) is how to combine \mathcal{F}_w and \mathcal{F}_d to construct \mathcal{Q} .

A. Codeword Allocation

According to the concatenated codebook structure, the adaptation of the codebook to the current χ can be done by finding the optimal combination of N_w and N_d . As shown in the previous section, when $\chi = 1$, setting $N = N_w$ (i.e., $\mathcal{Q} = \mathcal{F}_w$) is the optimal codeword allocation and when $\chi = 0$, setting $N = N_d$ (i.e., $\mathcal{Q} = \mathcal{F}_d$) is the optimal codeword allocation. The scenario when $0 < \chi < 1$ is the case where N_w and N_d are determined to minimize the bound (20).

In order to obtain solutions in closed-form, random vector quantization (RVQ) codebooks are employed to minimize the bound in (20). Using the RVQ results in [24] (Corollary 1) and [25] (Lemma 1), we can further get

$$G(\mathcal{Q}, \chi) \leq \sqrt{\chi} E[\lambda_{w,1}] N_w^{-\frac{1}{M_t-1}} + (1 - \sqrt{\chi}) E[\lambda_{d,1}] N_s^{-\frac{2}{M_t-2}} \quad (21)$$

where $N_s = \text{car}(\mathcal{F}_s)$ and $N_s = \frac{N_d}{2}$. Under the constraints $N = N_w + N_d$ and N_d is even, we find the combination of (N_w, N_d) to minimize (21). This optimization problem is formulated as

$$\begin{aligned} N_w = \underset{\tilde{N}_w}{\text{argmin}} &\left(\sqrt{\chi} E[\lambda_{w,1}] \tilde{N}_w^{-\frac{1}{M_t-1}} \right. \\ &\left. + (1 - \sqrt{\chi}) E[\lambda_{d,1}] (N - \tilde{N}_w)^{-\frac{2}{M_t-2}} 2^{\frac{2}{M_t-2}} \right) \quad (22) \end{aligned}$$

s.t. $N = \tilde{N}_w + \tilde{N}_d$, $\tilde{N}_w \geq 0$, $\tilde{N}_d \geq 0$, and \tilde{N}_d is even integer.

It is not difficult to show that the objective function (22) is convex on \tilde{N}_w . From (22), it is evident that when $\chi = 0$, the minimizer of the objective function in (22) is obtained at $\tilde{N}_w = 0$, and when $\chi = 1$, $\tilde{N}_w = N$ is the minimizer. The problem now is to find \tilde{N}_w that minimizes the objective function for $0 < \chi < 1$. By using standard Lagrangian optimization, we obtain the condition for the optimal N_w as

$$\left(\frac{1 - \sqrt{\chi} E[\lambda_{d,1}] M_t - 1}{\sqrt{\chi} E[\lambda_{w,1}] M_t - 2} N_w^{\frac{M_t}{M_t-1}} \right)^{\frac{M_t-2}{M_t}} = \frac{N - N_w}{2}. \quad (23)$$

Given M_t , M_r , and $0 < \chi < 1$, (23) can be solved through a numerical grid search as

$$\bar{N}_w = \operatorname{argmin}_{\hat{N}_w \in \mathcal{N}_w} \left| \frac{N - \hat{N}_w}{2} - \left(\frac{1 - \sqrt{\chi}}{\sqrt{\chi}} \frac{E[\lambda_{d,1}]}{E[\lambda_{w,1}]} \frac{M_t - 1}{M_t - 2} \hat{N}_w^{\frac{M_t}{M_t - 1}} \right)^{\frac{M_t - 2}{M_t}} \right| \quad (24)$$

where $\mathcal{N}_w = \{0, N/L, 2N/L, \dots, (L-1)N/L, N\}$ and L denotes the number of quantization levels. Then, the codeword allocation can be done by

$$N_w = \min \{ \lfloor \bar{N}_w \rfloor_2, N \} \quad (25)$$

and

$$N_d = N - N_w \quad (26)$$

where $\lfloor \cdot \rfloor_2$ denotes the flooring function to the nearest even integer. The quantization level L indicates how many codebooks with different combinations of (N_w, N_d) with $N = N_w + N_d$ are employed to perform the adaptation to the XPD.

Note that the grid search provides a convenient way of handling the case when the XPD is random or not initially known. In this case, the XPD statistic χ can be estimated by the receiver and one of the $L+1$ codeword allocations determined from the grid search can be sent as feedback overhead to the transmitter. We refer to this technique as *codebook switching*. Given the XPD and quantization level L , the adaptation is performed by choosing a codebook corresponding to the optimal codeword allocation pairs (N_w, N_d) among $L+1$ codebooks. Variation of the XPD results in a codebook switching within $L+1$ codebooks. For example, when $L = 1$, (25) and (26) allocate two codebooks $\mathcal{Q} = \mathcal{F}_w$ with $N = N_w$ and $\mathcal{Q} = \mathcal{F}_d$ with $N = N_d$ across the χ axis (i.e., codebook switching within $\{\mathcal{F}_w, \mathcal{F}_d\}$ depending on χ).

To evaluate (24), the values of $E[\lambda_{w,1}]$ and $E[\lambda_{d,1}]$ should be known. These can be computed numerically or can be obtained analytically by using the p.d.f. of the dominant eigenvalue of a Wishart matrix [18]. For deriving (25) and (26), the RVQ bounds $E\left[1 - \max_{\mathbf{f}_w \in \mathcal{F}_w} |\mathbf{v}_{w,1}^* \mathbf{f}_w|^2\right] \leq N_w^{-\frac{1}{M_t-1}}$ and $E\left[1 - \max_{\mathbf{f}_s \in \mathcal{F}_s} |\mathbf{v}_{s,1}^* \mathbf{f}_s|^2\right] \leq N_s^{-\frac{2}{M_t-2}}$ have been employed. For fixed M_t , in general, the RVQ bound is loose for small N and thereby produces loose estimation for N_w and N_d in (25) and (26). However, as N becomes larger, the RVQ bounds becomes tighter and the trend of the codeword allocation complies with the original distribution.

B. Asymptotic Analysis

In this subsection, we look at the trend of the codeword allocation in (25) and (26) in the large number of antennas regime. In [26], it has been shown that if M_t and M_r tend to infinity and the ratio $\frac{M_r}{M_t}$ converges to a certain bounded value $\alpha \in [0, 1]$ (i.e., $\lim_{M_t, M_r \rightarrow \infty} \frac{M_r}{M_t} = \alpha$), $\lambda_{w,1}$ satisfies

$$\lim_{M_t, M_r \rightarrow \infty} \frac{\lambda_{w,1}}{M_t} \stackrel{a.s.}{\rightarrow} (1 + \sqrt{\alpha})^2 \quad (27)$$

almost surely. Define $\mathbf{R}_{11} = \mathbf{H}_{11}^* \mathbf{H}_{11}$ and $\mathbf{R}_{22} = \mathbf{H}_{22}^* \mathbf{H}_{22}$. Then, by using (27), as M_t and M_r tend to infinity with $\frac{M_r}{M_t} \rightarrow \alpha$, the ratio $E[\lambda_{d,1}]/E[\lambda_{w,1}]$ in (23) converges to

$$\begin{aligned} \lim_{M_t, M_r \rightarrow \infty} \frac{E[\lambda_{d,1}]}{E[\lambda_{w,1}]} &= \lim_{M_t, M_r \rightarrow \infty} \frac{E[\max\{\lambda_1(\mathbf{R}_{11}), \lambda_1(\mathbf{R}_{22})\}]}{E[\lambda_{w,1}]} \\ &= \lim_{M_t, M_r \rightarrow \infty} \frac{E\left[\max\left\{\frac{\lambda_1(\mathbf{R}_{11})}{M_t/2}, \frac{\lambda_1(\mathbf{R}_{22})}{M_t/2}\right\}\right]}{2 E\left[\frac{\lambda_{w,1}}{M_t}\right]} \\ &\stackrel{a.s.}{=} \frac{1}{2} \frac{\max\{2(1+\sqrt{\alpha})^2, 2(1+\sqrt{\alpha})^2\}}{2(1+\sqrt{\alpha})^2} \quad (28) \\ &= \frac{1}{2} \quad (29) \end{aligned}$$

where the equality in (28) follows from the fact that $\frac{\lambda_{w,1}}{M_t} \stackrel{a.s.}{\rightarrow} 2(1+\sqrt{\alpha})^2$ and

$$\left\{ \frac{\lambda_1(\mathbf{R}_{11})}{M_t/2}, \frac{\lambda_1(\mathbf{R}_{22})}{M_t/2} \right\} \stackrel{a.s.}{\rightarrow} \{2(1+\sqrt{\alpha})^2, 2(1+\sqrt{\alpha})^2\}$$

almost surely.

Using the convergence result in (29), (23) becomes $(1 - \sqrt{\chi})/\sqrt{\chi} \stackrel{a.s.}{=} (N - \bar{N}_w)/\bar{N}_w$ almost surely. In this case, the codeword allocation becomes simply

$$N_w = \lfloor N\sqrt{\chi} \rfloor_2 \quad (30)$$

and

$$N_d = N - \lfloor N\sqrt{\chi} \rfloor_2. \quad (31)$$

The resulting codeword allocation in (30) and (31) implies that with an asymptotically large number of antennas, the optimal N_w minimizing (21) is given by the fraction of N where the fraction is determined by $\sqrt{\chi}$. Note that with a large number of antennas, regardless of the codebook size N , the same number of codewords are assigned to \mathcal{F}_w and \mathcal{F}_d at $\chi = 1/4$.

C. Concatenation

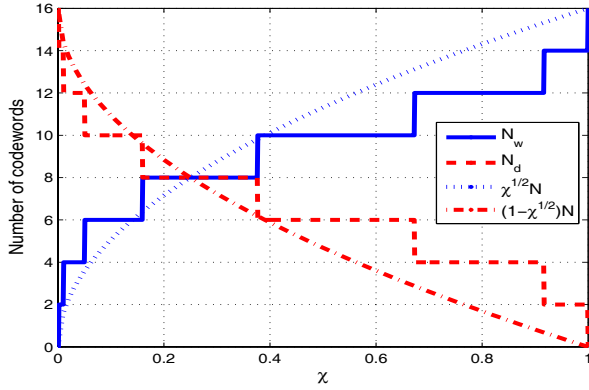
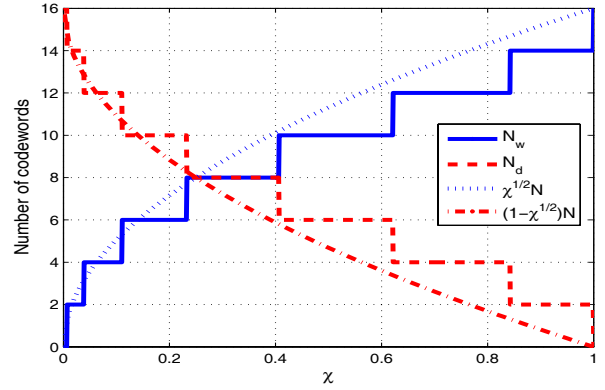
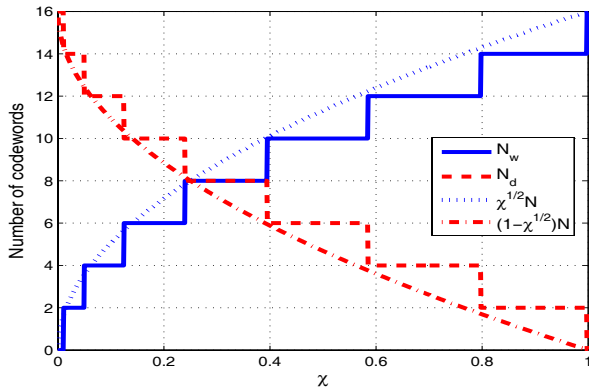
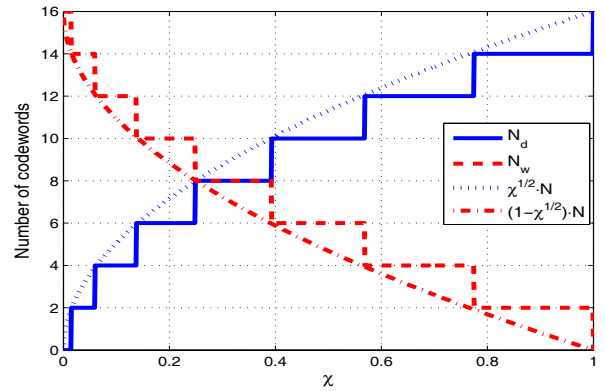
Once N_w and $N_s = N_d/2$ are determined according to (25) and (26), the codebooks \mathcal{F}_w and \mathcal{F}_s are designed to minimize the distortion upper bound in (20). Thus, $\mathcal{F}_w = \{\mathbf{f}_{w,1}, \mathbf{f}_{w,2}, \dots, \mathbf{f}_{w,N_w}\}$ is designed by maximizing the minimum distance between codewords in the M_t -dimensional Grassmannian manifold where the minimum distance is given by

$$\sigma(\mathcal{F}_w) = \min_{1 \leq i < j \leq N_w} \sqrt{1 - |\mathbf{f}_{w,i}^* \mathbf{f}_{w,j}|^2}. \quad (32)$$

Similarly, $\mathcal{F}_s = \{\mathbf{f}_{s,1}, \mathbf{f}_{s,2}, \dots, \mathbf{f}_{s,N_s}\}$ is designed by maximizing the minimum distance between codewords in the $M_t/2$ -dimensional Grassmannian manifold. The minimum distance is given by

$$\sigma(\mathcal{F}_s) = \min_{1 \leq i < j \leq N_s} \sqrt{1 - |\mathbf{f}_{s,i}^* \mathbf{f}_{s,j}|^2}. \quad (33)$$

As shown in Section IV, \mathcal{F}_d is generated by constructing the upper non-zero vector and lower non-zero vector, $\mathbf{f}_{du,i} = \begin{bmatrix} \mathbf{f}_{s,i}^T & \mathbf{0}_{M_t/2 \times 1}^T \end{bmatrix}^T$ and $\mathbf{f}_{dl,N_s+i} = \begin{bmatrix} \mathbf{0}_{M_t/2 \times 1}^T & \mathbf{f}_{s,i}^T \end{bmatrix}^T$ for $i = 1, 2, \dots, N_s$. Then, we get $\mathcal{F}_d = \{\mathcal{F}_{du}, \mathcal{F}_{dl}\} = \{\mathbf{f}_{du,1}, \dots, \mathbf{f}_{du,N_d/2}, \mathbf{f}_{dl,1}, \dots, \mathbf{f}_{dl,N_d/2}\}$.

(a) Codewords allocation for $N=16$ with $M_t=4$ and $M_r=2$.(b) Codewords allocation for $N=16$ with $M_t=8$ and $M_r=4$.(c) Codewords allocation for $N=16$ with $M_t=16$ and $M_r=8$.(d) Codewords allocation for $N=16$ with $M_t=64$ and $M_r=32$.Fig. 2. Codewords allocation between N_w and N_d for various combination of M_t and M_r .

Since \mathcal{F}_w and \mathcal{F}_d are designed independently, a direct concatenation $\{\mathcal{F}_w, \mathcal{F}_d\}$ would produce an undesirable codeword alignment such that $|\mathbf{f}_{w,i}^* \mathbf{f}_{d,j}| \approx 1$ for $\mathbf{f}_{w,i} \in \mathcal{F}_w$ and $\mathbf{f}_{d,j} \in \mathcal{F}_d$. In this case, the distinction between $\mathbf{f}_{w,i}$ and $\mathbf{f}_{d,j}$ in a metric space is not clear resulting in degradation in codebook performance. This problem is solved by designing the rotation matrix \mathbf{U} so that two codebooks $\mathbf{U}\mathcal{F}_w$ and \mathcal{F}_d are separated as far as possible, where \mathbf{U} is a M_t -dimensional unitary matrix. In other words, the concatenated codebook is designed as $\mathcal{Q} = \{\mathbf{U}\mathcal{F}_w, \mathcal{F}_d\}$ so that the unitary matrix \mathbf{U} maximizes the minimal distance between codewords in $\mathcal{Q} = \{\mathbf{q}_1, \mathbf{q}_2, \dots, \mathbf{q}_N\}$ by rotating the codebook \mathcal{F}_w , i.e.,

$$\mathbf{U} = \underset{\tilde{\mathbf{U}} \in \mathcal{U}(M_t, M_t)}{\operatorname{argmax}} \min_{1 \leq i < j \leq N} \sqrt{1 - |\mathbf{q}_i^* \mathbf{q}_j|^2}, \quad (34)$$

where $\mathcal{U}(M_t, M_t)$ denotes the set of all M_t -dimensional unitary matrices. In order to design \mathbf{U} , it is often most practical to employ a random computer search that improves the codebook iteratively by a *hill-climbing* strategy until convergence.

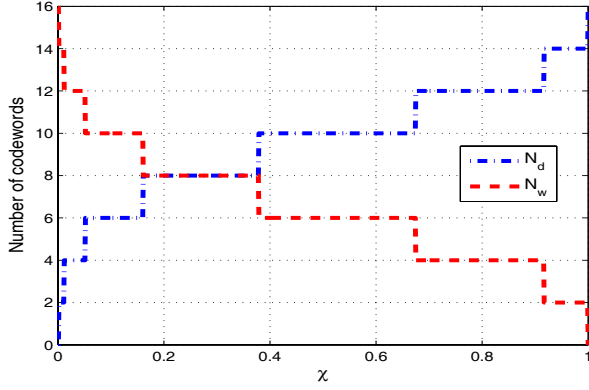
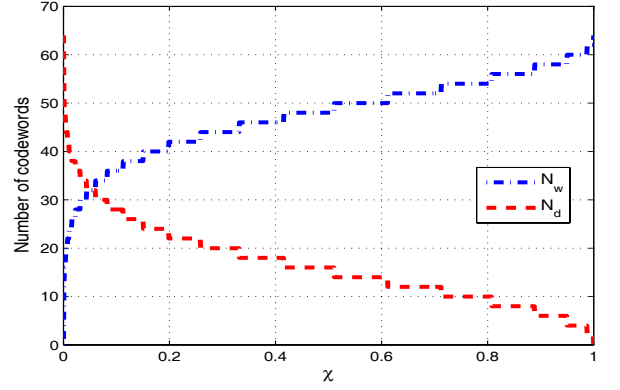
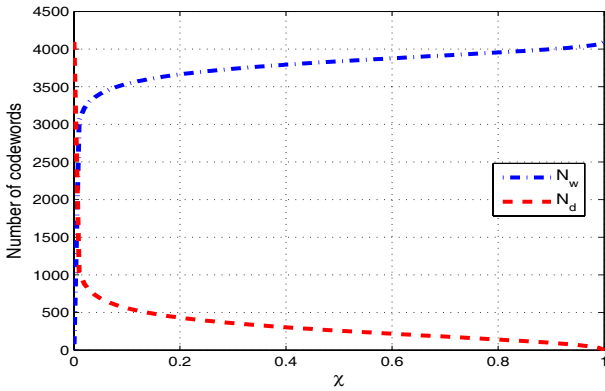
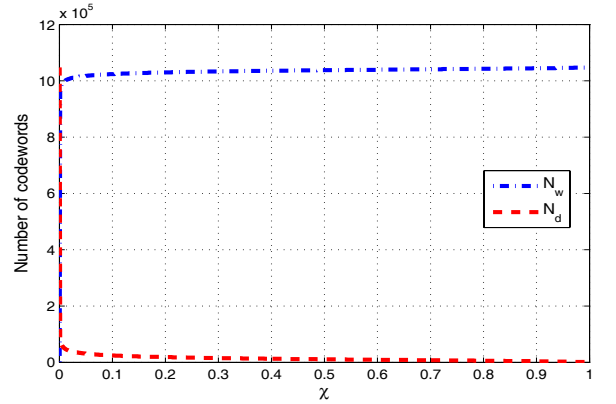
VI. SIMULATION RESULTS

In this section, we provide simulations to corroborate the results in the previous sections and also perform Monte Carlo

simulations to verify the average effective SNR performance and capacity performance of our limited feedback MIMO dual-polarized antennas system.

First, we look at how the codeword allocation should vary as χ evolves from 0 to 1. Fig. 2 shows the N_w and N_d combinations (i.e., (25) and (26)) for $N=16$ with different M_t and M_r . Note that in Fig. 2 the antenna dimension increases while maintaining the ratio $M_r/M_t = 1/2$ demonstrating the asymptotic behavior of the codeword allocation studied in Section V-B. From Figs. 2 (a) to (d), we can observe that the codeword allocation trend approaches the functions $\lfloor N\sqrt{\chi} \rfloor_2$ and $N - \lfloor N\sqrt{\chi} \rfloor_2$ for N_w and N_d , respectively, as M_t and M_r tend to infinity. As can be seen from Fig. 2 (c), the codeword allocation begins to be governed by the scaling law $N\sqrt{\chi}$ around $M_t=16$ and $M_r=8$. In Fig. 2 (c) and (d), the same number of codewords for \mathcal{F}_d and \mathcal{F}_w are assigned at $\chi = 1/4$, which corresponds to the analysis in Section V-B.

In the next simulation study, we observe the codeword allocation trend in the large codebook size regime. Fig. 3 displays the (N_w, N_d) combinations (i.e., (25) and (26)) with different N for $M_t=4$ and $M_r=2$. In Fig. 3, we can observe that as N increases, the transition regime where N_w changes

(a) Codewords allocation for $N=2^4$ with $M_t = 4$ and $M_r = 2$.(b) Codewords allocation for $N=2^6$ with $M_t = 4$ and $M_r = 2$.(c) Codewords allocation for $N=2^{12}$ with $M_t = 4$ and $M_r = 2$.(d) Codewords allocation for $N=2^{18}$ with $M_t = 4$ and $M_r = 2$.Fig. 3. Codewords allocation between N_w and N_d for various number of codebook size N .

from 0 to N is concentrated around $\chi = 0$. To understand this behavior, define a specific point χ_ϵ on χ axis, where at χ_ϵ the equality in (23) holds as $N_w = \frac{N}{1+\epsilon}$. Here, ϵ is any value in $(0, \infty)$. By plugging $N_w = \frac{N}{1+\epsilon}$ in (23) and after some algebraic manipulation, the equality (23) yields

$$\left(\frac{1 - \sqrt{\chi_\epsilon} E[\lambda_{d,1}] M_t - 1}{\sqrt{\chi_\epsilon} E[\lambda_{w,1}] M_t - 2} \right)^{\frac{M_t-2}{M_t}} = \frac{1}{2} \left(\frac{N \epsilon^{M_t-1}}{1+\epsilon} \right)^{\frac{1}{M_t-1}}.$$

This expression implies that for fixed M_t and any $\epsilon \in (0, \infty)$, as N tends infinity (respectively, N tends zero), the χ_ϵ approaches 0 (respectively, χ_ϵ approaches 1). The fact that $\chi_\epsilon \rightarrow 0$ as $N \rightarrow \infty$ for an arbitrary $0 < \epsilon < \infty$ reveals that as $N \rightarrow \infty$ all the values $N_w \in (0, N)$ are concentrated around the point $\chi_\epsilon = 0$ due to the definition $N_w = \frac{N}{1+\epsilon}$ and the convergence $\chi_\epsilon \rightarrow 0$. Therefore, asymptotically with N , the codebook is $\mathcal{Q} = \mathcal{F}_w$ for $0 < \chi \leq 1$ and $\mathcal{Q} = \mathcal{F}_d$ for $\chi = 0$. With the concatenated codebook structure $\mathcal{Q} = \{\mathcal{F}_w, \mathcal{F}_d\}$ where \mathcal{F}_w is M_t -dimensional Grassmannian line packing (GLP) codebook and \mathcal{F}_d is the block diagonal codebook, the M_t -dimensional GLP codebook is the optimal codebook almost everywhere on χ as N tend infinity. As can be seen from Fig. 3, this trend is observed when the system

employs over 18 bits of feedback. Note that the purpose of this simulation is to gain intuition about the codeword allocation in the large codebook regime and not as a demonstration of practicality.

As mentioned in the last paragraph of Section V-A, the codeword allocation in (25) and (26) does not cope with the original distribution, since the RVQ bound is loose for small N . However, for large N , we can expect the derived codeword split will comply with original distribution because of its tightness for large N such that $\log_2(N) \gg M_t$. Fig. 4 shows a comparison between the codeword allocation based on the RVQ bound (21) and the codeword allocation obtained numerically from the original distortion (8) for $M_t = M_r = 4$ and $N = 64, 256$. For the simulated curves, we ran Monte Carlo simulations over 50,000 iterations on the χ axis with interval $[0, 1]$. For each iteration, $N = 64$ and $N = 256$ RVQ codebooks with all possible combinations (N_w, N_d) are generated randomly and evaluated. As can be seen from Fig. 4, the codeword allocation in (25) and (26) with 6 bits of feedback roughly follows the original distribution. Eight bits of feedback shows close agreement to the original distribution.

To verify the quality of the designed codebook based on

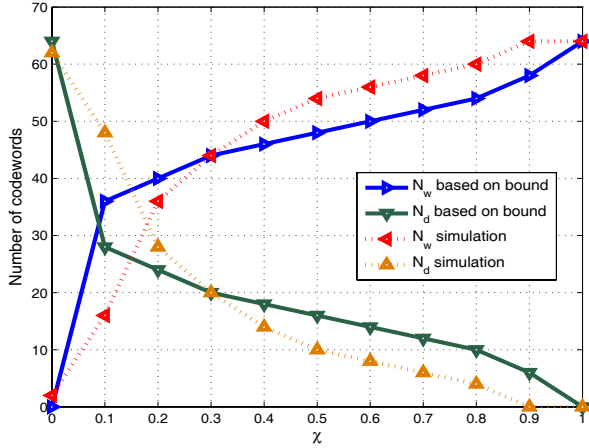
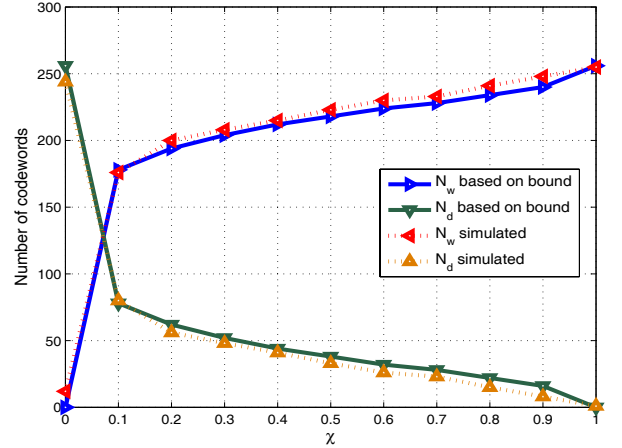
(a) $M_t = M_r = 4$ and $N = 64$.(b) $M_t = M_r = 4$ and $N = 256$.

Fig. 4. Comparison between proposed codeword allocation and codeword allocation based on the original distribution for $M_t = M_r = 4$, $N = 64$ and $N = 256$.

the bound (20) we compare the average SNR distortion of our codebook with that of a Lloyd codebook. Note that the Lloyd codebook is designed to minimize SNR distortion in (8) directly. Five Lloyd codebooks are designed at $\chi \in \{0, 0.25, 0.5, 0.75, 1.0\}$ for $N = 16$ and $N = 64$.² For the proposed concatenated codebook, $L = 4$ for $N = 16$ and $L = 5$ for $N = 64$ are used where L denotes the number of quantization level in searching grid $\mathcal{N}_w = \{0, N/L, 2N/L, \dots, (L-1)N/L\}$ of the concatenated codebook. As can be seen from Fig. 5, the proposed codebook based on the bound (20) does not deviate much from the performance of the Lloyd codebook. Specifically, when $N = 64$, both show similar performance. This demonstrates that the structured codebook obtained from the bound in (20) with an optimal codeword allocation provides comparable performance with the Lloyd codebook. This also reveals that the bounds (12) and (20) closely models the original SNR distortion (8).

In this simulation study, we investigate how much benefit is obtained by using the concatenated codebook rather than \mathcal{F}_w with $N_w = N$ or \mathcal{F}_d with $N_d = N$. Throughout the simulation 4×4 dual-polarized MIMO channel is assumed. In Fig. 6 and Fig. 7, the average SNR distortion (8) and capacity of the concatenated codebook, GLP codebook, and block diagonal codebook across χ axis are displayed. In Fig. 7, the SNR ρ is fixed at 15 dB. For generating $N = 16$ and $N = 64$ concatenated codebooks, $L = 4$ and $L = 5$ are employed, which results in 5 and 6 codebooks with different (N_w, N_d) combinations, respectively. We can check that the average SNR performance correctly characterizes the capacity performance. When $N = 64$, the concatenated codebook with

²If designed with enough iterations, the Lloyd codebook is nearly optimal. However, the convergence speed of the algorithm depends on initial centroids. For this reason, the Lloyd codebook for a specific χ value is obtained by choosing the best codebook from 5 candidate codebooks. Each candidate codebook is acquired by running the Lloyd algorithm independently with random initial centroids.

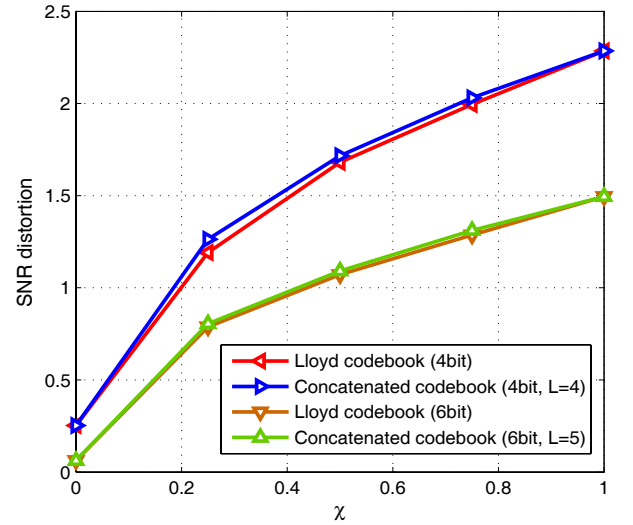
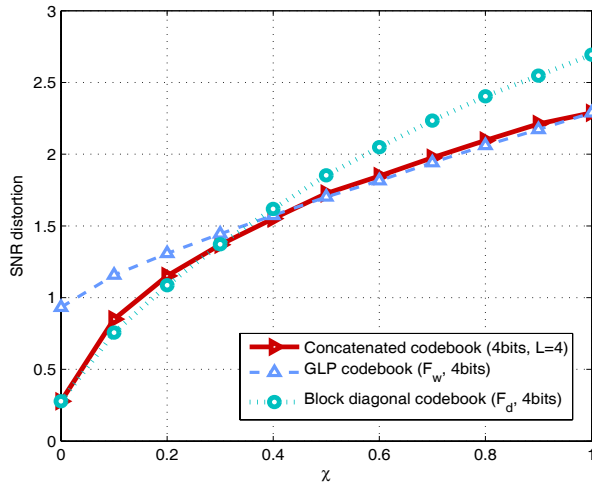
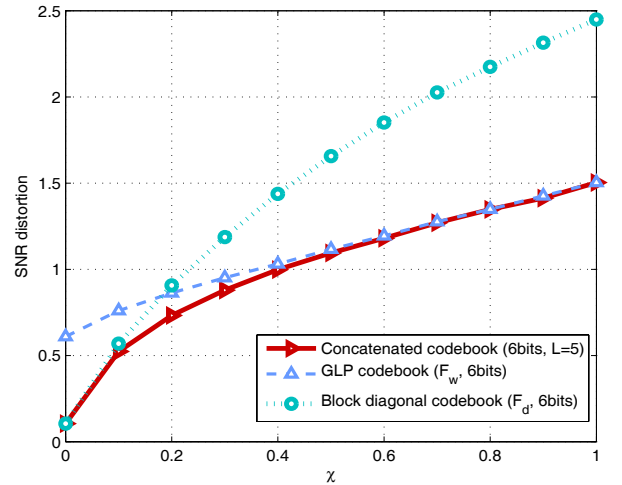
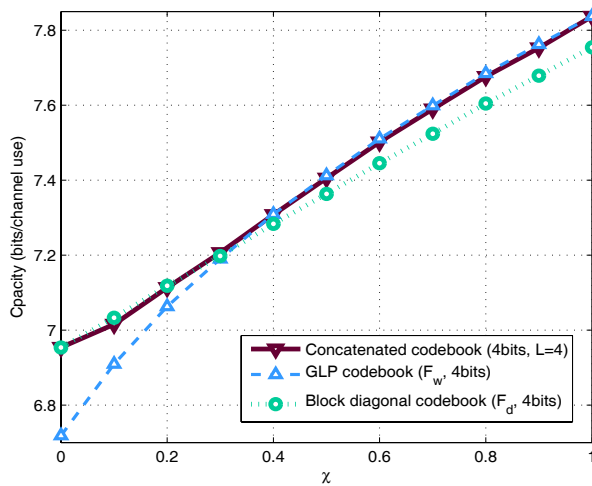
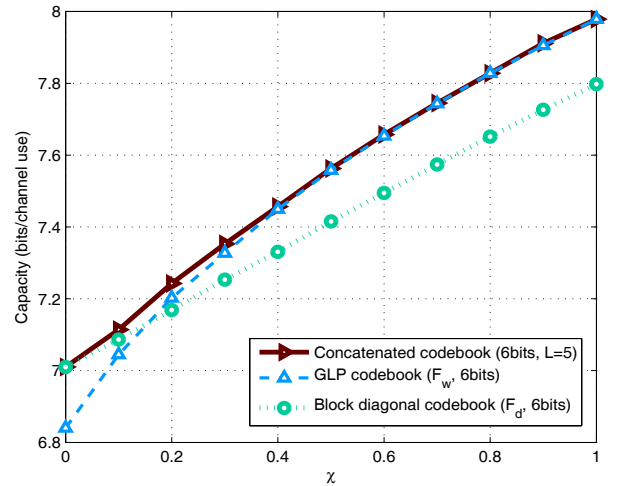


Fig. 5. SNR distortion comparison between Lloyd codebook and concatenated codebook for $M_t = M_r = 4$, $N = 16$, and 64.

6 codebook switching yields lower distortion than \mathcal{F}_w and \mathcal{F}_d over all χ values. The χ parameter has an inverse relation with XPD, and in [6], [7], it is reported that the XPD of dual-polarized channel has a large mean value (between 15 dB and 5 dB, which correspond to $\chi = 0.0316$ and $\chi = 0.3162$) in most scenarios. This fact and the simulation study in Fig. 6 and Fig. 7 demonstrate that the proposed codebook can achieve a large capacity benefit compared to the codebook designed for single-polarized antennas. We compare the performance at $\rho = 15$ dB. However, this trend does not alter even at low ρ due to the monotonicity of the log function.

In the previous simulations, the results are shown for $\chi = [0, 1]$. In the next simulation study, we evaluate the performance of the concatenated codebook across XPD (dB)

(a) $M_t = M_r = 4$ and $N = 16$.(b) $M_t = M_r = 4$ and $N = 64$.Fig. 6. Average SNR distortion comparison between concatenated codebook, GLP codebook, and block diagonal codebook across χ axis.(a) $M_t = M_r = 4$, SNR = 15 dB, and $N = 16$.(b) $M_t = M_r = 4$, SNR = 15 dB, and $N = 64$.Fig. 7. Average capacity performance comparison between concatenated codebook, GLP codebook, and block diagonal codebook across χ axis.

values. Fig. 8 displays the average SNR distortion (8) and capacity performance. We assume $M_t = M_r = 4$ and $N = 64$ and ρ is fixed at 15 dB for the capacity plot. The XPD is chosen to vary from 0 dB ($\chi = 1$) to 15 dB ($\chi = 0.031$). As can be seen from the figure, the performance trend in Fig. 6 and Fig. 7 does not change. Next, to provide more practical evaluations, we used XPD values generated by the space-time channel model (SCM) [6] in the urban micro environment. Note that in SCM [6], the XPD value is generated based on real measurement data. The average SNR distortion and capacity performance averaged over all XPD values are shown in Fig. 9 and Fig. 10 across different numbers of feedback bits. We assume $M_t = M_r = 4$ and $\rho = 15$ dB for the

capacity plot. In every channel use, a new XPD value is produced by the SCM and the performance is evaluated and averaged. Concatenated codebooks for 2 bits ($L = 2$), 4 bits ($L = 4$), 6 bits ($L = 5$), and 8 bits ($L = 10$) of feedback are generated. In addition to these codebooks, we generate another set of concatenated codebooks switching only between \mathcal{F}_w and \mathcal{F}_d (i.e., $L = 1$) for 2, 4, 6, and 8 bits of feedback. As the number of feedback bits increases, the performance improvement of the block diagonal codebook becomes inferior to the other codebooks. The concatenated codebook shows the best performance where the gain mainly comes from the ability to switch adaptively between $L+1$ different codebooks with different codeword allocations. Even for two codebook

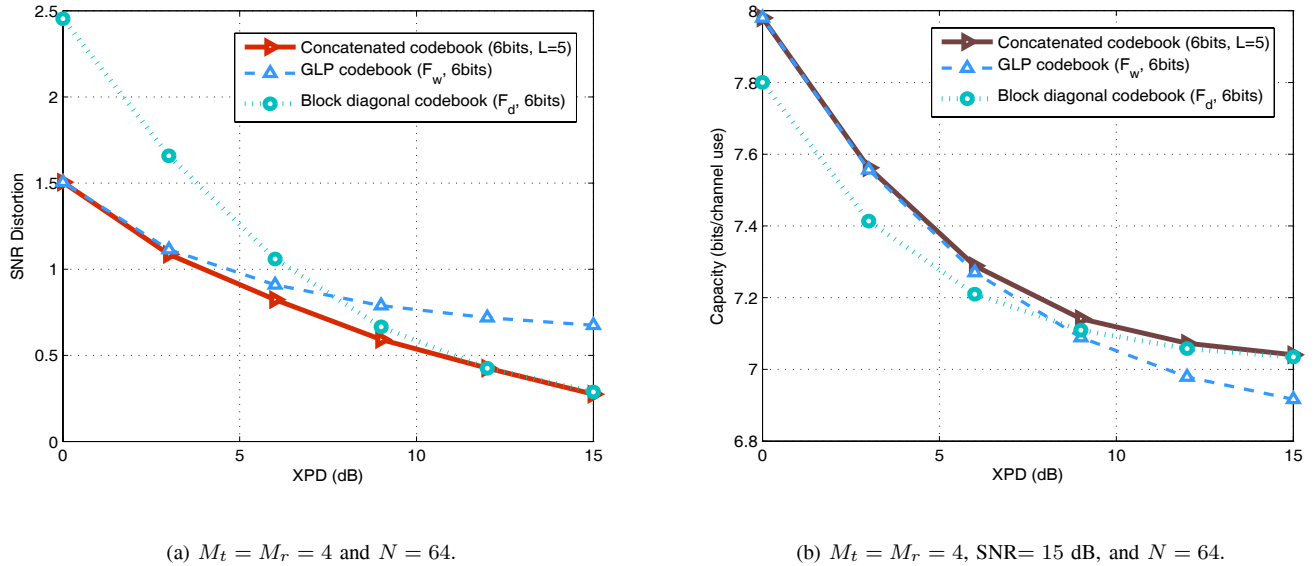


Fig. 8. Average SNR and capacity performance comparison between concatenated codebook, GLP codebook, and block diagonal codebook across XPD (dB) axis.

switching (i.e., $L = 1$), the proposed codebook offers better performance than the GLP codebook for all numbers of feedback bits and provides significant gain compared to the block diagonal codebooks especially at 6 and 8 bits of feedback.

VII. DISCUSSION AND CONCLUSIONS

We proposed a framework for performing limited feedback beamforming over dual-polarized MIMO channels using a codebook known to both the transmitter and receiver. Based on average SNR performance analysis, an upper bound on the average SNR distortion was found as a weighted sum of two beamforming distortion metrics corresponding to the single polarized channel and the block diagonal channel. By applying RVQ analysis, the distortion minimization problem can be solved by allocating a different number of codewords for two beamforming distortion metrics as a function of the channel XPD. Simulations show the proposed codebook switching scheme can provide moderate capacity gain in dual-polarized MIMO channel.

An important point we did not discuss is the implementation required to realize the proposed codebook switching scheme. To implement the proposed scheme, $L + 1$ concatenated codebooks must be designed offline and the mapping table from χ to a concatenated codebook must be stored at the transmitter and the receiver. Note that in order to design the concatenated codebook, we need to compute (24) for each χ values using numerical grid search. If the grid search is too complicated, one can simply impose \bar{N}_w to be a real value and get \bar{N}_w by using Newton's method or another iterative numerical algorithm [27]. In a large dimensional system, we can simply use (30) and (31) as an approximation to the grid search. When we perform limited feedback beamforming this kind of offline complexity is not of much concern. Once the $L+1$ concatenated codebooks and the mapping table are stored at the transmitter and the receiver, the online (or run-time)

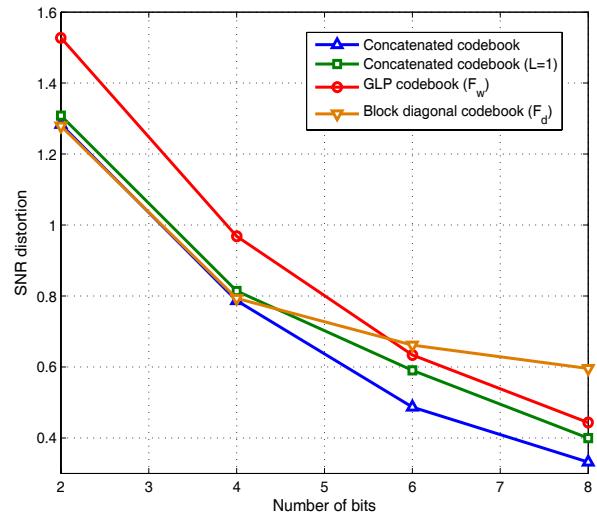


Fig. 9. Average SNR distortion comparison between concatenated codebook, GLP codebook, and block diagonal codebook across number of feedback bits.

complexity consists of feedback overhead related to both the long term statistic χ and instantaneous beamforming index. Since the overhead of feeding back the long term statistic χ is negligible compared to the overhead for feeding back the beamforming index, the proposed scheme requires the same operational complexity with the conventional limited feedback beamforming framework.

Switching the codebook can be done in a long term manner since the XPD is a long term statistic. Thus, the overhead caused by switching the codebook is negligible. Here, switching the codebook can be seen as performing *codebook adaptation* based on long term statistics (the codebook is changed once the long term statistics vary) as supported in

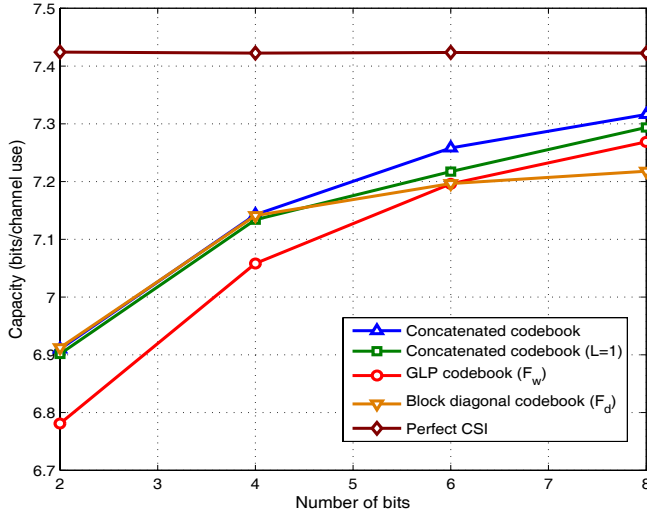


Fig. 10. Average capacity comparison between concatenated codebook, GLP codebook, and block diagonal codebook across number of feedback bits.

IEEE 802.16m [28]. In addition, IEEE 802.16m [28] supports another mode of codebook switching between 4 bit and 6 bit codebooks for 4 transmit antennas. Codebook switching is also a practical approach for 3GPP-LTE [29] where a codebook subset restriction is supported. The codebook subset restriction is used to prevent the receiver from feeding back a codeword which is useless (i.e., in a correlated environment). The transmitter and receiver switch to another subset codebook whenever it is required.

One additional cost of deploying the system would be the storage overhead for saving $L+1$ multiple codebooks. Using a constrained (or finite) alphabet structure for the codebook like 3GPP LTE [29] makes storage easy and simplifies channel quality indicator (CQI) calculation. In addition, given a codeword allocation N_w and N_d , constructing the concatenated codebook $\mathcal{Q} = \{\mathcal{F}_w, \mathcal{F}_d\}$ by choosing each \mathcal{F}_w and \mathcal{F}_d in supercodebooks such that $\mathcal{F}_w \subset \mathcal{S}_w$ with $\text{car}(\mathcal{S}_w) = N$ and $\mathcal{F}_d \subset \mathcal{S}_d$ with $\text{car}(\mathcal{S}_d) = N$ can avoid storing $L+1$ codebooks. The rotation matrix \mathbf{U} can alternatively be designed by maximizing the minimum distance of the codebook $\{\mathbf{U}\mathcal{S}_w, \mathcal{S}_d\}$. Practical standards such as 3GPP LTE [29] and IEEE 802.16m [28] support this kind of subset selection for constructing the codebook.

Thus, from the above arguments, the overall overhead required to deploy the proposed scheme is approximately the same as the overhead for conventional systems (e.g., 3GPP LTE and IEEE 802.16m). Therefore, the gain obtained using the proposed codebook can have practical impact.

Another point that we did not address in detail is the effect of channel imperfection. For example, when channel correlation exists the bounds in (14) and (15) do not hold because the eigenvalues and eigenvectors of the channel \mathbf{H}_w and \mathbf{H}_d are no longer independent. Despite these difficulties, one can derive average SNR distortion bounds similar to (14) and (15) using the results in [15]. The only difference is the scaling factor attached to eigenvalues. This reveals that despite channel correlation, one can still design a codebook

\mathcal{F}_w and \mathcal{F}_d as in the i.i.d. case. The adaptation of \mathcal{F}_w and \mathcal{F}_d to correlation statistics may be done by using projection technique in [14] or by designing spherical cap codebook in [15].

One limitation of the proposed work is that we only considered the codebook design for a single data stream. The dual-polarized channel can support multiple data streams through orthogonal polarizations achieving polarization diversity. A natural extension of our work would be to design a higher rank codebook by combining block diagonal matrices (or rotated block diagonal matrices) and full matrices so that the minimum chordal distance of the combined codebook is maximized. This has been initially explored in [16]. A more explicit adaptation to XPD is possible by determining the number of column subsets from the block diagonal matrix codewords and full matrix codewords based on channel statistics. Constructing an adaptive codebook switching scheme in spatial multiplexing is an interesting topic for future work.

APPENDIX A PROOF OF LEMMA 1

We prove that

$$\lambda_1(\mathbf{H}_\chi^* \mathbf{H}_\chi) \leq \|\mathbf{H}_{\chi+\Delta} \mathbf{v}_{\chi,1}\|_2^2, \quad (35)$$

where the vector $\mathbf{v}_{\chi,1} \in \mathbb{C}^{M_t \times 1}$ denotes the dominant eigenvector of $\mathbf{H}_\chi^* \mathbf{H}_\chi$. From (10) and (11), we can expand $\mathbf{H}_{\chi+\Delta}^* \mathbf{H}_{\chi+\Delta}$ as

$$\begin{aligned} \mathbf{H}_{\chi+\Delta}^* \mathbf{H}_{\chi+\Delta} &= \mathbf{H}_d^* \mathbf{H}_d + \chi(1+\Delta)^2 \mathbf{H}_{od}^* \mathbf{H}_{od} + \sqrt{\chi}(1+\Delta) \mathbf{R}_c \\ &= \mathbf{H}_\chi^* \mathbf{H}_\chi + \Delta [\chi(\Delta+2) \mathbf{H}_{od}^* \mathbf{H}_{od} + \sqrt{\chi} \mathbf{R}_c], \end{aligned} \quad (36)$$

where $\mathbf{R}_c = \mathbf{H}_d^* \mathbf{H}_{od} + \mathbf{H}_{od}^* \mathbf{H}_d$. By expanding $\|\mathbf{H}_{\chi+\Delta} \mathbf{v}_{\chi,1}\|_2^2$ with (36), we have

$$\begin{aligned} \|\mathbf{H}_{\chi+\Delta} \mathbf{v}_{\chi,1}\|_2^2 &= \lambda_1(\mathbf{H}_\chi^* \mathbf{H}_\chi) + \Delta [\chi(\Delta+2) \|\mathbf{H}_{od} \mathbf{v}_{\chi,1}\|_2^2 \\ &\quad + \sqrt{\chi} \mathbf{v}_{\chi,1}^* \mathbf{R}_c \mathbf{v}_{\chi,1}]. \end{aligned} \quad (37)$$

In order to show (35), we need to show the second term on the r.h.s. of (37) is positive. Since the \mathbf{R}_c is not a positive-semidefinite matrix, concluding that the second term is positive is not clear. However, (37) can be rewritten as

$$\begin{aligned} \|\mathbf{H}_{\chi+\Delta} \mathbf{v}_{\chi,1}\|_2^2 &= \lambda_1(\mathbf{H}_\chi^* \mathbf{H}_\chi) + \Delta [\chi(\Delta+1) \|\mathbf{H}_{od} \mathbf{v}_{\chi,1}\|_2^2 \\ &\quad + \lambda_1(\mathbf{H}_\chi^* \mathbf{H}_\chi) - \|\mathbf{H}_d \mathbf{v}_{\chi,1}\|_2^2], \end{aligned} \quad (38)$$

where in (38) we use the equality that

$$\lambda_1(\mathbf{H}_\chi^* \mathbf{H}_\chi) - \|\mathbf{H}_d \mathbf{v}_{\chi,1}\|_2^2 = \chi \|\mathbf{H}_{od} \mathbf{v}_{\chi,1}\|_2^2 + \sqrt{\chi} \mathbf{v}_{\chi,1}^* \mathbf{R}_c \mathbf{v}_{\chi,1}.$$

This equality is obtained by expanding $\mathbf{v}_{\chi,1}^* \mathbf{H}_\chi^* \mathbf{H}_\chi \mathbf{v}_{\chi,1}$ using (10). Let us focus on the two terms $\lambda_1(\mathbf{H}_\chi^* \mathbf{H}_\chi) - \|\mathbf{H}_d \mathbf{v}_{\chi,1}\|_2^2$ on the r.h.s. of (38). Clearly, $\|\mathbf{H}_d \mathbf{v}_{\chi,1}\|_2^2 \leq \lambda_1(\mathbf{H}_d^* \mathbf{H}_d)$, and it is evident that $\lambda_1(\mathbf{H}_{11}^* \mathbf{H}_{11}) \leq \lambda_1(\mathbf{H}_\chi^* \mathbf{H}_\chi)$ and $\lambda_1(\mathbf{H}_{22}^* \mathbf{H}_{22}) \leq \lambda_1(\mathbf{H}_\chi^* \mathbf{H}_\chi)$ due to the inclusion principle [30]. Since the dominant eigenvalue of $\mathbf{H}_d^* \mathbf{H}_d$ is the maximum value of $\lambda_1(\mathbf{H}_{11}^* \mathbf{H}_{11})$ and $\lambda_1(\mathbf{H}_{22}^* \mathbf{H}_{22})$, we obtain the relation

$$\begin{aligned} \|\mathbf{H}_d \mathbf{v}_{\chi,1}\|_2^2 &\leq \lambda_1(\mathbf{H}_d^* \mathbf{H}_d) \\ &= \max\{\lambda_1(\mathbf{H}_{11}^* \mathbf{H}_{11}), \lambda_1(\mathbf{H}_{22}^* \mathbf{H}_{22})\} \\ &\leq \lambda_1(\mathbf{H}_\chi^* \mathbf{H}_\chi), \end{aligned} \quad (39)$$

which implies $\lambda_1(\mathbf{H}_\chi^* \mathbf{H}_\chi) - \|\mathbf{H}_d \mathbf{v}_{\chi,1}\|_2^2 \geq 0$. Since $\lambda_1(\mathbf{H}_\chi^* \mathbf{H}_\chi) - \|\mathbf{H}_d \mathbf{v}_{\chi,1}\|_2^2 \geq 0$ and (38) holds for arbitrary small $\Delta \geq 0$, we conclude that $\lambda_1(\mathbf{H}_\chi^* \mathbf{H}_\chi) \leq \|\mathbf{H}_{\chi+\Delta} \mathbf{v}_{\chi,1}\|_2^2$ (i.e., (35)). Since $\|\mathbf{H}_{\chi+\Delta} \mathbf{v}_{\chi,1}\|_2^2 \leq \lambda_1(\mathbf{H}_{\chi+\Delta}^* \mathbf{H}_{\chi+\Delta})$, we finally get the result

$$\lambda_1(\mathbf{H}_\chi^* \mathbf{H}_\chi) \leq \lambda_1(\mathbf{H}_{\chi+\Delta}^* \mathbf{H}_{\chi+\Delta}). \quad (40)$$

Eqn. (40) holds for arbitrary small Δ . This concludes the proof.

APPENDIX B PROOF OF LEMMA 2

Define $\mathbf{f}' = \operatorname{argmax}_{\mathbf{f} \in \mathcal{F}} \|\mathbf{H}_\chi \mathbf{f}\|_2^2$. We first claim that

$$E \left[\|\mathbf{H}_\chi \mathbf{f}'\|_2^2 \right] \leq E \left[\|\mathbf{H}_{\chi+\Delta} \mathbf{f}'\|_2^2 \right]. \quad (41)$$

By using the same procedures employed in (36) to (38) with \mathbf{f}' instead of $\mathbf{v}_{\chi,1}$, we have

$$E \left[\|\mathbf{H}_{\chi+\Delta} \mathbf{f}'\|_2^2 \right] = E \left[\|\mathbf{H}_\chi \mathbf{f}'\|_2^2 \right] + \Delta \left[\chi (\Delta + 1) E \left[\|\mathbf{H}_{od} \mathbf{f}'\|_2^2 \right] + E \left[\|\mathbf{H}_\chi \mathbf{f}'\|_2^2 \right] - E \left[\|\mathbf{H}_d \mathbf{f}'\|_2^2 \right] \right]. \quad (42)$$

Let us focus on the two terms $E \left[\|\mathbf{H}_\chi \mathbf{f}'\|_2^2 \right] - E \left[\|\mathbf{H}_d \mathbf{f}'\|_2^2 \right]$ on the r.h.s. of (42). In order to show (41), it is sufficient to verify that $E \left[\|\mathbf{H}_\chi \mathbf{f}'\|_2^2 \right] - E \left[\|\mathbf{H}_d \mathbf{f}'\|_2^2 \right] \geq 0$. The term $\|\mathbf{H}_\chi \mathbf{f}'\|_2^2$ can be equivalently written and lower-bounded by

$$\begin{aligned} \|\mathbf{H}_\chi \mathbf{f}'\|_2^2 &= \max_{\mathbf{f} \in \mathcal{F}} \left\{ \|\mathbf{H}_d \mathbf{f}\|_2^2 + \chi \|\mathbf{H}_{od} \mathbf{f}\|_2^2 + \sqrt{\chi} \mathbf{f}^* \mathbf{R}_c \mathbf{f} \right\} \quad (43) \\ &\geq \|\mathbf{H}_d \mathbf{f}^\dagger\|_2^2 + \chi \|\mathbf{H}_{od} \mathbf{f}^\dagger\|_2^2 + \sqrt{\chi} (\mathbf{f}^\dagger)^* \mathbf{R}_c \mathbf{f}^\dagger \quad (44) \end{aligned}$$

where $\mathbf{f}^\dagger = \operatorname{argmax}_{\mathbf{f} \in \mathcal{F}} \|\mathbf{H}_d \mathbf{f}\|_2^2$. Then,

$E \left[\|\mathbf{H}_\chi \mathbf{f}'\|_2^2 \right] - E \left[\|\mathbf{H}_d \mathbf{f}'\|_2^2 \right]$ is lower bounded by

$$\begin{aligned} E \left[\|\mathbf{H}_\chi \mathbf{f}'\|_2^2 - \|\mathbf{H}_d \mathbf{f}'\|_2^2 \right] &\geq E \left[\|\mathbf{H}_\chi \mathbf{f}'\|_2^2 - \|\mathbf{H}_d \mathbf{f}^\dagger\|_2^2 \right] \quad (45) \\ &\geq E \left[\chi \|\mathbf{H}_{od} \mathbf{f}^\dagger\|_2^2 + \sqrt{\chi} (\mathbf{f}^\dagger)^* \mathbf{R}_c \mathbf{f}^\dagger \right], \quad (46) \end{aligned}$$

where in (45) the fact $\|\mathbf{H}_d \mathbf{f}'\|_2^2 \leq \|\mathbf{H}_d \mathbf{f}^\dagger\|_2^2$ is used. In (46), the lower bound (44) is applied to the term $E \left[\|\mathbf{H}_\chi \mathbf{f}'\|_2^2 \right]$ on the r.h.s. of (45). Now, the expectation of $\|\mathbf{H}_{od} \mathbf{f}^\dagger\|_2^2$ in (46) is $E \left[\|\mathbf{H}_{od} \mathbf{f}^\dagger\|_2^2 \right] = \frac{M_r}{2}$, because the \mathbf{f}^\dagger is independent of \mathbf{H}_{od} (i.e., \mathbf{f}^\dagger is chosen regardless of \mathbf{H}_{od}). The \mathbf{f}^\dagger in $E \left[(\mathbf{f}^\dagger)^* \mathbf{R}_c \mathbf{f}^\dagger \right]$ in (46) is dependent on \mathbf{H}_d in \mathbf{R}_c , where $\mathbf{R}_c = \mathbf{H}_d^* \mathbf{H}_{od} + \mathbf{H}_{od}^* \mathbf{H}_d$. Using the conditional expectation, we obtain

$$E_{\mathbf{f}^\dagger} \left[(\mathbf{f}^\dagger)^* E_{\mathbf{H}_w | \mathbf{f}^\dagger} [\mathbf{R}_c] \mathbf{f}^\dagger \right] = 0, \quad (47)$$

because $E_{\mathbf{H}_w | \mathbf{f}^\dagger} [\mathbf{R}_c] = \mathbf{0}$. Thus, the quantity $E \left[\|\mathbf{H}_{\chi+\Delta} \mathbf{f}'\|_2^2 \right]$ in (42) is lower bounded by

$$\begin{aligned} E \left[\|\mathbf{H}_{\chi+\Delta} \mathbf{f}'\|_2^2 \right] &\geq E \left[\|\mathbf{H}_\chi \mathbf{f}'\|_2^2 \right] \\ &\quad + \Delta \left[\chi (\Delta + 1) E \left[\|\mathbf{H}_{od} \mathbf{f}'\|_2^2 \right] + \chi \frac{M_r}{2} \right]. \quad (48) \end{aligned}$$

Since (48) holds for arbitrary $\Delta \geq 0$, this shows the relation (41). Since $E \left[\|\mathbf{H}_{\chi+\Delta} \mathbf{f}'\|_2^2 \right] \leq E \left[\max_{\mathbf{f} \in \mathcal{F}} \|\mathbf{H}_{\chi+\Delta} \mathbf{f}\|_2^2 \right]$, we obtain the desired result

$$E \left[\max_{\mathbf{f} \in \mathcal{F}} \|\mathbf{H}_\chi \mathbf{f}\|_2^2 \right] \leq E \left[\max_{\mathbf{f} \in \mathcal{F}} \|\mathbf{H}_{\chi+\Delta} \mathbf{f}\|_2^2 \right]. \quad (49)$$

Eqn. (49) holds for arbitrary small Δ . This concludes the proof.

APPENDIX C PROOF OF THEOREM 1

First, we claim for any unit norm vector $\mathbf{u} \in \mathbb{C}^{M_t \times 1}$, the quantity $\|\mathbf{H}_\chi \mathbf{u}\|_2^2$ is convex on $\sqrt{\chi}$. Convexity can be checked by verifying the nonnegativity of the second order derivative of $\|\mathbf{H}_\chi \mathbf{u}\|_2^2$ w.r.t $\sqrt{\chi}$. With $\|\mathbf{H}_\chi \mathbf{u}\|_2^2 = \|\mathbf{H}_d \mathbf{u}\|_2^2 + \chi \|\mathbf{H}_{od} \mathbf{u}\|_2^2 + \sqrt{\chi} \mathbf{u}^* \mathbf{R}_c \mathbf{u}$, we have $\frac{\partial^2 \|\mathbf{H}_\chi \mathbf{u}\|_2^2}{(\partial \sqrt{\chi})^2} = 2 \|\mathbf{H}_{od} \mathbf{u}\|_2^2 \geq 0$, which implies the convexity of $\|\mathbf{H}_\chi \mathbf{u}\|_2^2$ on $\sqrt{\chi}$.

Now, we claim that the $G(\mathcal{F}, \chi)$ is also convex on $\sqrt{\chi}$. With the Voronoi region partition, we can rewrite

$$E \left[\lambda_1(\mathbf{H}_\chi^* \mathbf{H}_\chi) \right] = \sum_{n=1}^N P_{\chi,n} E_{\mathbf{H}_\chi | \mathbf{H}_\chi \in \mathcal{V}_{\chi,n}} \left[\sup_{\|\mathbf{u}\|_2=1} \|\mathbf{H}_\chi \mathbf{u}\|_2^2 \right] \quad (50)$$

and

$$E \left[\max_{\mathbf{f} \in \mathcal{F}} \|\mathbf{H}_\chi \mathbf{f}_\chi\|_2^2 \right] = \sum_{n=1}^N P_{\chi,n} (\mathbf{f}_n^* E_{\mathbf{H}_\chi | \mathbf{H}_\chi \in \mathcal{V}_{\chi,n}} [\mathbf{H}_\chi^* \mathbf{H}_\chi] \mathbf{f}_n) \quad (51)$$

where $P_{\chi,n} = \operatorname{Prob}(\mathbf{H}_\chi \in \mathcal{V}_{\chi,n})$. Then, using (50) and (51), $G(\mathcal{F}, \chi)$ is given by

$$G(\mathcal{F}, \chi) = \sum_{n=1}^N P_{\chi,n} E_{\mathbf{H}_\chi | \mathbf{H}_\chi \in \mathcal{V}_{\chi,n}} [\varphi(\mathbf{H}_\chi)] \quad (52)$$

where

$$\varphi(\mathbf{H}_\chi) = \sup_{\|\mathbf{u}\|_2=1} \left[\|\mathbf{H}_\chi \mathbf{u}\|_2^2 - \mathbf{f}_n^* E_{\mathbf{H}_\chi | \mathbf{H}_\chi \in \mathcal{V}_{\chi,n}} [\mathbf{H}_\chi^* \mathbf{H}_\chi] \mathbf{f}_n \right]. \quad (53)$$

Now, conditioned on $\mathbf{H}_\chi \in \mathcal{V}_{\chi,n}$, $\varphi(\mathbf{H}_\chi)$ in (52) is convex on $\sqrt{\chi}$, because the pointwise maximum over the infinite set of convex functions (i.e., $\sup_{\|\mathbf{u}\|_2=1} \|\mathbf{H}_\chi \mathbf{u}\|_2^2$) is convex on $\sqrt{\chi}$

conditioned on the fixed value $\mathbf{f}_n^* E_{\mathbf{H}_\chi | \mathbf{H}_\chi \in \mathcal{V}_{\chi,n}} [\mathbf{H}_\chi^* \mathbf{H}_\chi] \mathbf{f}_n$. The conditional expectation $E_{\mathbf{H}_\chi | \mathbf{H}_\chi \in \mathcal{V}_{\chi,n}} [\varphi(\mathbf{H}_\chi)]$ in (52) represents the nonnegative weighted infinite summation (i.e., integral) of $\varphi(\mathbf{H}_\chi)$, which preserves the convexity on $\sqrt{\chi}$. Now, Eqn. (52) is the nonnegative weighted finite summation of $E_{\mathbf{H}_\chi | \mathbf{H}_\chi \in \mathcal{V}_{\chi,n}} [\varphi(\mathbf{H}_\chi)]$ over the partition $\mathcal{V}_{\chi,n}$ for $n = 1, 2, \dots, N$, which still preserves the convexity on χ . Thus, we can conclude that $G(\mathcal{F}, \chi)$ is a convex function on $\sqrt{\chi}$.

Next, we must prove the monotonicity of $G(\mathcal{F}, \chi)$. The convexity of $G(\mathcal{F}, \chi)$ on $\sqrt{\chi}$ implies that the increasing rate of (50) is larger than or equal to that of (51) as $\sqrt{\chi}$ increases. Thus, $G(\mathcal{F}, \chi)$ is always monotonically increasing on $[0, 1]$ as $\sqrt{\chi}$ increases if and only if $G'(\mathcal{F}, 0) = \frac{\partial}{\partial \sqrt{\chi}} G(\mathcal{F}, \chi) |_{\sqrt{\chi}=0} \geq 0$. In the sequel, we are going to verify that $G'(\mathcal{F}, 0) \geq 0$.

We first need to show the existence of $G'(\mathcal{F}, \chi)$ on $[0, 1]$, where $G'(\mathcal{F}, \chi)$ is given by

$$G'(\mathcal{F}, \chi) = \frac{\partial E \left[\lambda_1(\mathbf{H}_\chi^* \mathbf{H}_\chi) \right]}{\partial \sqrt{\chi}} - \frac{\partial E \left[\max_{\mathbf{f} \in \mathcal{F}} \|\mathbf{H}_\chi \mathbf{f}\|_2^2 \right]}{\partial \sqrt{\chi}}.$$

Due to the almost everywhere differentiability of a monotone function [31] and the monotonicity of $E[\lambda_1(\mathbf{H}_\chi^* \mathbf{H}_\chi)]$ and $E\left[\max_{\mathbf{f} \in \mathcal{F}} \|\mathbf{H}_\chi \mathbf{f}\|_2^2\right]$ on $[0, 1]$ (i.e., Lemma 1 and Lemma 2), the differentiation of $G(\mathcal{F}, \chi)$ w.r.t. $\sqrt{\chi}$ is well defined. This implies that with probability 1, there exists $G'(\mathcal{F}, \chi)$ on $[0, 1]$. Now, we are ready to show that $G'(\mathcal{F}, 0) \geq 0$.

For an arbitrarily small $\delta > 0$, the function $G(\mathcal{F}, \delta)$ is given by

$$G(\mathcal{F}, \delta) = E\left[\|\mathbf{H}_\delta \mathbf{v}_{\delta,1}\|_2^2 - \left(\max_{\mathbf{f} \in \mathcal{F}} \|\mathbf{H}_\delta \mathbf{f}\|_2^2\right)\right],$$

where $\mathbf{v}_{\delta,1}$ denotes the dominant eigenvector of $\mathbf{H}_\delta^* \mathbf{H}_\delta$. Then, the first order derivative of $G(\mathcal{F}, \chi)$ on $\sqrt{\chi} = 0$ (i.e., $G'(\mathcal{F}, 0) = \lim_{\delta \rightarrow 0} \frac{G(\mathcal{F}, \delta) - G(\mathcal{F}, 0)}{\delta}$) can be equivalently written and lower bounded as shown at the top of the next page.

In (54), the inequalities $\|\mathbf{H}_\delta \mathbf{v}_{\delta,1}\|_2^2 \geq \|\mathbf{H}_\delta \mathbf{v}_{d,1}\|_2^2$ and $\max_{\mathbf{f} \in \mathcal{F}} \|\mathbf{H}_d \mathbf{f}\|_2^2 \geq \left\|\mathbf{H}_d \mathbf{f}_\delta^\dagger\right\|_2^2$, where $\mathbf{f}_\delta^\dagger = \operatorname{argmax}_{\mathbf{f} \in \mathcal{F}} \|\mathbf{H}_d \mathbf{f}\|_2^2$ are used. Now, using the equalities

$$\begin{aligned} \|\mathbf{H}_\delta \mathbf{v}_{d,1}\|_2^2 - \|\mathbf{H}_d \mathbf{v}_{d,1}\|_2^2 &= \delta^2 \|\mathbf{H}_{od} \mathbf{v}_{d,1}\|_2^2 + \delta \mathbf{v}_{d,1}^* \mathbf{R}_c \mathbf{v}_{d,1} \\ \left\|\mathbf{H}_\delta \mathbf{f}_\delta^\dagger\right\|_2^2 - \left\|\mathbf{H}_d \mathbf{f}_\delta^\dagger\right\|_2^2 &= \delta^2 \left\|\mathbf{H}_{od} \mathbf{f}_\delta^\dagger\right\|_2^2 + \delta (\mathbf{f}_\delta^\dagger)^* \mathbf{R}_c \mathbf{f}_\delta^\dagger, \end{aligned}$$

we can further get from (54)

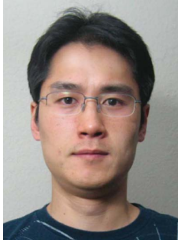
$$\begin{aligned} G'(\mathcal{F}, 0) &\geq \lim_{\delta \rightarrow 0} E\left[\delta \|\mathbf{H}_{od} \mathbf{v}_{d,1}\|_2^2 - \left(\delta \left\|\mathbf{H}_{od} \mathbf{f}_\delta^\dagger\right\|_2^2 + (\mathbf{f}_\delta^\dagger)^* \mathbf{R}_c \mathbf{f}_\delta^\dagger\right)\right] \\ &= \lim_{\delta \rightarrow 0} E\left[-(\mathbf{f}_\delta^\dagger)^* \mathbf{R}_c \mathbf{f}_\delta^\dagger\right] \\ &= 0. \end{aligned} \quad (56)$$

In (55), we set $\mathbf{v}_{d,1}^* \mathbf{R}_c \mathbf{v}_{d,1} = 0$ because \mathbf{R}_c is an off-block diagonal matrix and the dominant eigenvector of $\mathbf{H}_d^* \mathbf{H}_d$ has either an upper non-zero or a lower non-zero structure. In (56), we use the property that as $\delta \rightarrow 0$, $\mathbf{f}_\delta^\dagger$ becomes independent of \mathbf{H}_{od} , which results in $\lim_{\delta \rightarrow 0} E\left[(\mathbf{f}_\delta^\dagger)^* \mathbf{R}_c \mathbf{f}_\delta^\dagger\right] = 0$ (i.e., (47) in Lemma 2). Thus, we have that $G'(\mathcal{F}, 0) \geq 0$, which asserts that $G(\mathcal{F}, \chi)$ is a monotonic increasing function of $\sqrt{\chi}$.

REFERENCES

- [1] D. Gesbert, M. Shafi, D. Shiu, P. Smith, and A. Naguib, "From theory to practice: an overview of MIMO space-time coded wireless systems," *IEEE J. Sel. Areas Commun.*, vol. 21, no. 3, pp. 281–301, Apr. 2003.
- [2] C. Oestges, V. Erceg, and A. J. Paulraj, "Propagation modeling of MIMO multipolarized fixed wireless channels," *IEEE Trans. Veh. Technol.*, vol. 53, no. 4, pp. 644–654, May 2004.
- [3] P. Soma, D. S. Baum, V. Erceg, R. Krishnamoorthy, and A. J. Paulraj, "Analysis and modeling of multiple-input multiple-output radio channels based on outdoor measurements conducted at 2.5 GHz for fixed BWA applications," in *Proc. IEEE Int. Conf. on Commun.*, Apr. 2002.
- [4] R. U. Nabar, H. Bolcskei, V. Erceg, D. Gesbert, and A. J. Paulraj, "Performance of multiantenna signaling techniques in the presence of polarization diversity," *IEEE Trans. Signal Process.*, vol. 50, no. 10, pp. 2553–2562, Oct. 2002.
- [5] M. Coldrey, "Modeling and capacity of polarized MIMO channel," in *Proc. IEEE Veh. Tech. Conf. Spring*, May 2008.
- [6] G. Calcev, D. Chizhik, B. Goransson, S. Howard, H. Huang, A. Kogiantis, A. F. Molisch, A. L. Moustakas, and H. X. D. Reed, "A wideband spatial channel model for system-wide simulations," *IEEE Trans. Veh. Technol.*, vol. 56, no. 2, pp. 389–403, Mar. 2007.
- [7] H. Asplund, J. Berg, F. Harrysson, J. Medbo, and M. Riback, "Propagation characteristics of polarized radio waves in cellular communications," in *Proc. IEEE Veh. Tech. Conf. Fall*, Sept. 2007.
- [8] A. Scaglione, P. Stoica, S. Barbarossa, G. B. Giannakis, and H. Sampath, "Optimal designs for space-time linear precoders and decoders," *IEEE Trans. Signal Process.*, vol. 50, no. 5, pp. 1051–1064, May 2002.
- [9] D. J. Love, R. W. Heath Jr., V. K. N. Lau, D. Gesbert, B. D. Rao, and M. Andrews, "An overview of limited feedback wireless communication systems," *IEEE J. Sel. Areas Commun.*, vol. 26, no. 8, pp. 1341–1365, Oct. 2008.
- [10] A. Narula, M. J. Lopez, M. D. Trott, and G. W. Wornell, "Efficient use of side information in multiple-antenna data transmission over fading channels," *IEEE J. Sel. Areas Commun.*, vol. 16, no. 8, pp. 1423–1436, Oct. 1998.
- [11] K. K. Mukkavilli, A. Sabharwal, E. Erkip, and B. Aazhang, "On beamforming with finite rate feedback in multiple-antenna systems," *IEEE Trans. Inf. Theory*, vol. 49, no. 10, pp. 2562–2579, Oct. 2003.
- [12] D. J. Love, R. W. Heath Jr., and T. Strohmer, "Grassmannian beamforming for multiple-input multiple-output wireless systems," *IEEE Trans. Inf. Theory*, vol. 49, no. 10, pp. 2735–2747, Oct. 2003.
- [13] P. Xia and G. B. Giannakis, "Design and analysis of transmit beamforming based on limited-rate feedback," *IEEE Trans. Signal Process.*, vol. 54, no. 5, pp. 1853–1863, May 2006.
- [14] D. J. Love and R. W. Heath Jr., "Limited feedback diversity techniques for correlated channels," *IEEE Trans. Veh. Technol.*, vol. 55, no. 2, pp. 713–722, Mar. 2006.
- [15] V. Raghavan, R. W. Heath Jr., and A. M. Sayeed, "Systematic codebook designs for quantized beamforming in correlated MIMO channels," *IEEE J. Sel. Areas Commun.*, vol. 25, no. 7, pp. 1298–1310, Sep. 2007.
- [16] B. Clerckx, Y. Zhou, and S. Kim, "Practical codebook design for limited feedback spatial multiplexing," *Proc. IEEE Int. Conf. on Commun.*, May 2008.
- [17] T. Kim, B. Clerckx, D. J. Love, and S. J. Kim, "Limited feedback beamforming codebook design for dual-polarized MIMO channel," in *Proc. IEEE Globecom*, Dec. 2008.
- [18] P. A. Dighe, R. K. Mallik, and S. S. Jamuar, "Analysis of transmit-receive diversity in Rayleigh fading," *IEEE Trans. Commun.*, vol. 51, no. 4, pp. 694–703, Apr. 2003.
- [19] M. K. Simon and M.-S. Alouini, *Digital Communications over Fading Channels*. New York: Wiley, 2000.
- [20] C. Oestges and B. Clerckx, *MIMO Wireless Communications: From Real-World Propagation to Space-Time Code Design*. Oxford, UK: Academic Press (Elsevier), 2007.
- [21] L. Jiang, L. Thiele, and V. Jungnickel, "On the modelling of polarized MIMO channel," in *Proc. Europ. Wireless (Paris)*, Apr. 2007.
- [22] M. Shafi, M. Zhang, A. L. Moustakas, P. J. Smith, A. F. Molisch, F. Tufvesson, and S. H. Simon, "Polarized MIMO channel in 3-d: models, measurements and mutual information," vol. 24, no. 3, pp. 514–527, Mar. 2006.
- [23] A. Tulino, A. Lozano, and S. Verdú, "Impact of antennas correlation on the capacity of multiantenna channels," *IEEE Trans. Inf. Theory*, vol. 51, no. 7, pp. 2491–2509, 2005.
- [24] C. K. Au-Yeung and D. J. Love, "On the performance of random vector quantization limited feedback beamforming in a MISO system," *IEEE Trans. Wireless Commun.*, vol. 6, no. 2, pp. 458–462, Feb. 2007.
- [25] N. Jindal, "MIMO broadcast channels with finite-rate feedback," *IEEE Trans. Inf. Theory*, vol. 52, no. 11, pp. 5045–5060, Nov. 2006.
- [26] A. Edelman, "Eigenvalues and condition numbers of random matrices," doctoral thesis, M.I.T., May 1989.
- [27] D. Kincaid and W. Cheney, *Numerical Analysis*, 3rd edition. Brooks/Cole, 2000.
- [28] "IEEE P802.16m-2008 draft standard for local and metropolitan area network," in IEEE Standard 802.16m, 2008.
- [29] "3GPP LTE Release-8 V0.0.9: Evolved Packet System RAN Part," in 3GPP LTE, Dec. 2009.
- [30] R. Horn and C. Johnson, *Matrix Analysis*. Cambridge, UK: Cambridge University Press, 1985.
- [31] A. Torchinsky, *Real Variables*, 1st edition. Westview Press, 1998.

$$\begin{aligned}
G'(\mathcal{F}, 0) &= \lim_{\delta \rightarrow 0} \frac{E \left[\|\mathbf{H}_\delta \mathbf{v}_{\delta,1}\|_2^2 - \max_{\mathbf{f} \in \mathcal{F}} \|\mathbf{H}_\delta \mathbf{f}\|_2^2 - \left(\|\mathbf{H}_d \mathbf{v}_{d,1}\|_2^2 - \max_{\mathbf{f} \in \mathcal{F}} \|\mathbf{H}_d \mathbf{f}\|_2^2 \right) \right]}{\delta} \\
&= \lim_{\delta \rightarrow 0} \frac{E \left[\|\mathbf{H}_\delta \mathbf{v}_{\delta,1}\|_2^2 - \|\mathbf{H}_d \mathbf{v}_{d,1}\|_2^2 - \left(\max_{\mathbf{f} \in \mathcal{F}} \|\mathbf{H}_\delta \mathbf{f}\|_2^2 - \max_{\mathbf{f} \in \mathcal{F}} \|\mathbf{H}_d \mathbf{f}\|_2^2 \right) \right]}{\delta} \\
&\geq \lim_{\delta \rightarrow 0} \frac{E \left[\|\mathbf{H}_\delta \mathbf{v}_{d,1}\|_2^2 - \|\mathbf{H}_d \mathbf{v}_{d,1}\|_2^2 - \left(\|\mathbf{H}_\delta \mathbf{f}_\delta^\dagger\|_2^2 - \|\mathbf{H}_d \mathbf{f}_d^\dagger\|_2^2 \right) \right]}{\delta}.
\end{aligned} \tag{54}$$



Taejoon Kim (S'08) received the B.S. degree (with highest honors) in electrical engineering from Sogang University, Seoul, Korea, in 2002, and M.S. degree in electrical engineering from the Korea Advanced Institute of Science and Technology (KAIST), Daejeon, Korea, in 2004. He is currently working towards the Ph.D. degree at Purdue University. He was a Summer Intern in DSPS R&D Center, Texas Instrument, Dallas, TX, in 2010 and in the Samsung R&D Center, Richardson, TX, in 2008, respectively. From 2004 to 2006, he was with

Electronics and Telecommunications Research Institute (ETRI), Daejeon, Korea. His research interests are in the design of adaptive communication systems.



Bruno Clerckx received the M.S. and Ph.D. degree in applied science from the Universite Catholique de Louvain, Belgium. He held visiting research positions at Stanford University, USA, and Eurecom Institute, France. He is currently with Samsung Advanced Institute of Technology, Samsung Electronics, Korea. He is the author or coauthor of one book on MIMO wireless communications and about 50 research papers. He has been actively contributing to 3GPP LTE/LTE-Advanced and IEEE 802.16m since 2007.



David J. Love (S'98 - M'05 - SM'09) received the B.S. (with highest honors), M.S.E., and Ph.D. degrees in electrical engineering from the University of Texas at Austin, in 2000, 2002, and 2004, respectively. During the summers of 2000 and 2002, he was with the Texas Instruments DSPS R&D Center, Dallas, TX. Since August 2004, he has been with the School of Electrical and Computer Engineering, Purdue University, West Lafayette, IN, where he is now an Associate Professor. Dr. Love has served as a Guest Editor for the IEEE JOURNAL ON SELECTED

AREAS IN COMMUNICATIONS and serves as an Associate Editor for the IEEE TRANSACTIONS ON COMMUNICATIONS. His research interests are in the design and analysis of communication systems. Dr. Love is a member of Tau Beta Pi and Eta Kappa Nu. In 2003, he received the IEEE Vehicular Technology Society Daniel Noble Fellowship.



Sungjin Kim was born in Korea in 1969. He received his doctor of philosophy (Ph.D.) degree in school of electrical engineering and computer science, Seoul national university. He got his master and bachelor of engineering degree in electronics and communications engineering from the college of engineering, Hanyang university, Korea in 2000 and in 1994, respectively. He has been working for 3GPP mobile communications standardization since 2000. His research interests include MIMO signal processing and wireless communications for bio and

medical equipments.